TECHNISCHE UNIVERSITÄT WIEN
Vienna University of Technology

DIPLOMA THESIS

Strategic oxidations on the Lanosterol core and sidechain towards rearranged *spiro-lanostanes*

By

Nicolas Heinzig, BSc

Supervised by

Ao.Univ.Prof. Dipl.-Ing. Dr.techn. Peter Gärtner

and

Projektass. Dipl.-Ing. Dr.rer.nat. Nicolas Kratena, BSc

Submitted at the

Institute of Applied Synthetic Chemistry

at TU Wien

“If the doors of perception were cleansed every thing would appear to man as it is, Infinite. For man has closed himself up, till he sees all things thro' narrow chinks of his cavern.”

— William Blake, The Marriage of Heaven and Hell

Acknowledgements

In writing this work I would like to express my deepest gratitude to…

… Dr Peter Gärtner for the possibility to work in his research group and for the instructive and patient advice during our group seminars.

… My supervisor Dr Nicolas Kratena for his experienced advice and the offer to work on this interesting and challenging project

… my lab mates Dr David Schachamayr, Dr Maximilian Kaiser and Dr Philipp Gritsch for offering assistance, interesting talks and scientific community

… my parents for always being there for me and offering me support in my education and career.

… my friends for cheering me up, helping me recreate in my free time and for believing in me.

Table of contents

1 Introduction

Triterpenoids – From *spiro*-Lanostanes to Forrestiacids

Triterpenoids constitute a large and diverse class of natural products with numerous biological activities. Their basic feature is a 30-carbon skeleton which is the result of a concerted cyclization event of a squalene precursor. The very controlled, enzyme-guided cyclizations enable many different termination events, hydride and alkyl shifts as well as rearrangements, which is causative for the structural diversity of triterpenoids. As a consequence, they are commonly sub-divided into various classes defined by their basic carbon framework. One of the most common is the lanostane scaffold, derived from Lanosterol (**1**) (see Figure 1) . It consists of an annealed 6/6/6/5-tetracycle with a carbon sidechain at C17. A great variety of natural products from various plants, fungi and maritime organisms belong to the lanostane group. Among them are a number of compounds that are of interest for medicinal and pharmaceutical research. [1]

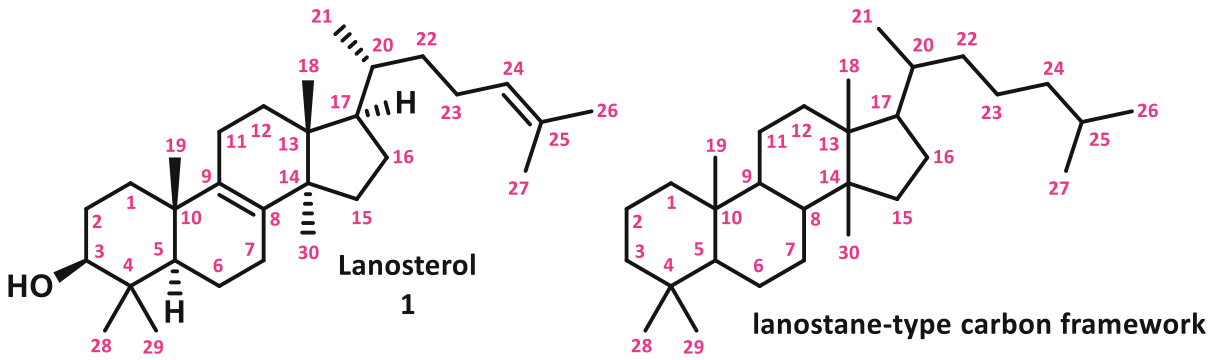

Figure 1: Lanosterol and its carbon skeleton with complete set of locants

Some of those compounds feature intriguing modifications of the lanostane skeleton. Ganotropic acid (**2**), isolated from the chinese mushroom species *Ganoderma tropicum*, contains a modified sidechain forming a ketal-like spirolactone. [2] Even more remarkable are the Urceoloids A (**3**) and B (**4**), which contain a rearranged carbon-skeleton forming a spirocycle out of the rings A and B. The rearranged skeleton of **3** and **4** can be traced back to a Wagner-Meerwein rearrangement of a hypothetical lanostane type precursor. [3]

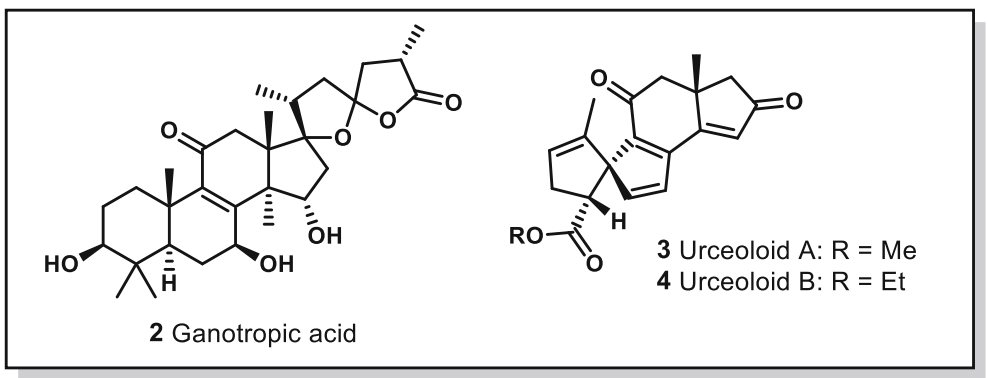

Figure 2: Selected lanostane type natural products containing spirocycles

Forrestiacids are a recently discovered group of pentaterpenoids derived from a lanostane type triterpenoid and the diterpenoid Levopimaric acid (**8**). The first isolated representatives Forrestiacids A (**5**) and B (**6**) were reported by Xiong et al. in 2021. Their most impressive structural feature is the rare [2.2.2]bicyclooctane moiety where the di- and triterpenoid units join. They could be extracted from the Chinese conifer *Pseudotsuga Forrestii*, along with Neoabiestrine F, an already known triterpenoid that serves as the likely precursor of Forrestiacids A (**5**) and B (**6**), forming a heterodimeric [4+2]-adduct with Levopimaric acid (**8**) in a Diels-Alder reaction. Out of 15 kg of dried leaves and twigs of *P. Forrestii*, the researchers were able to extract 1.2 g of Forrestiacid A (**5**), the *endo* product of the Diels-Alder reaction, as the major product, and only 100 mg of Forrestiacid B (**6**). [4]

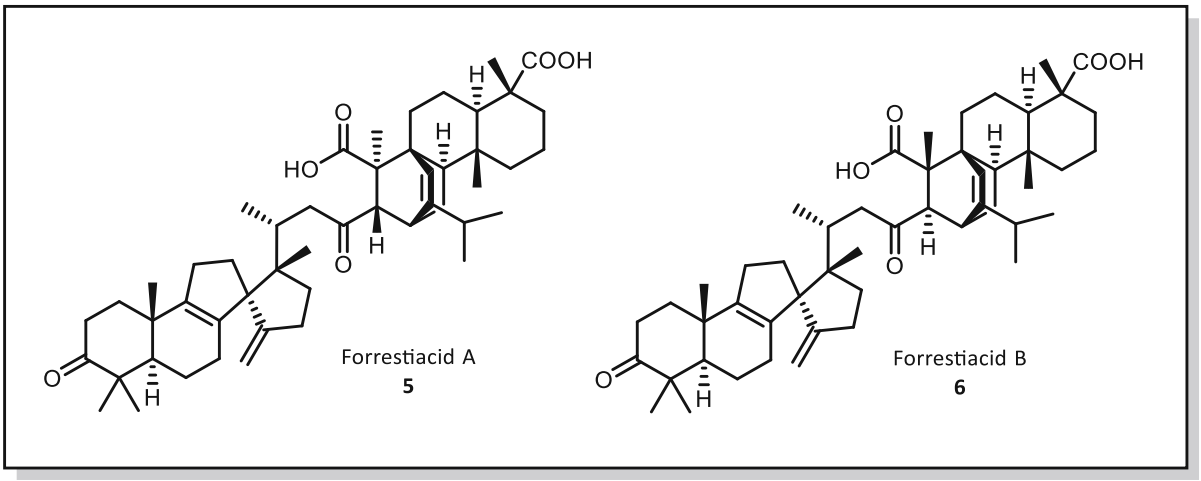

Figure 3: Forrestiacids A and B

The isolation of Neoabiestrine F (**7**) as a precursor with known structure was of great help in the elucidation of their structure. The stereochemical assignment of C24 and C25 was assisted by ROESY NMR experiments and further consolidated by Gauge Independent Atomic Orbital (GIAO) method ^{1}H and ^{13}C chemical shift calculations. Both Forrestiacids A (**5**) and B (**6**) have been shown to exert significant inhibition of the acyl-CoA citrate lyase (ACL), a key enzyme in fatty acid and cholesterol biosynthesis. The major component, Forrestiacid A (**5**) was also submitted to a *de-novo* lipogenesis assay where it showed considerable inhibition of fatty acid as well as cholesterol biosynthesis. [4]

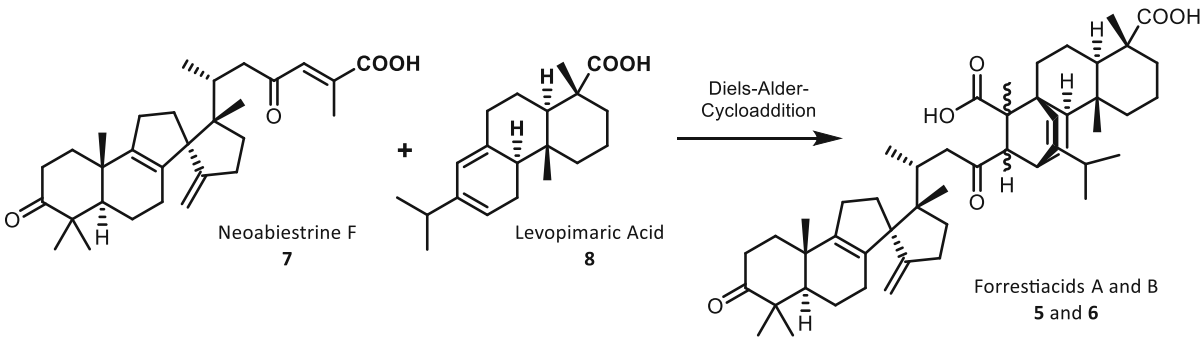

Scheme 1: Diels-Alder-Cycloaddition forming Forrestiacids A and B

Forrestiacids A (**5**) and B (**6**) are hypothesized to be derived from co-occurring Neoabiestrine F (**7**). The reaction of Neoabiestrine (**7**) with the abietadiene diterpenoid Levopimaric acid (= abieta-8(14),12-dien-18-oic acid) (**8**) to form Forrestiacids A and B is depicted in Scheme 1.

Neoabiestrine (**7**) itself can be derived from Firmanic acid (**9**) through the rearrangement of rings C and D to form a [5.5]-spirocycle as Scheme 2 illustrates. [4][5][6][7]

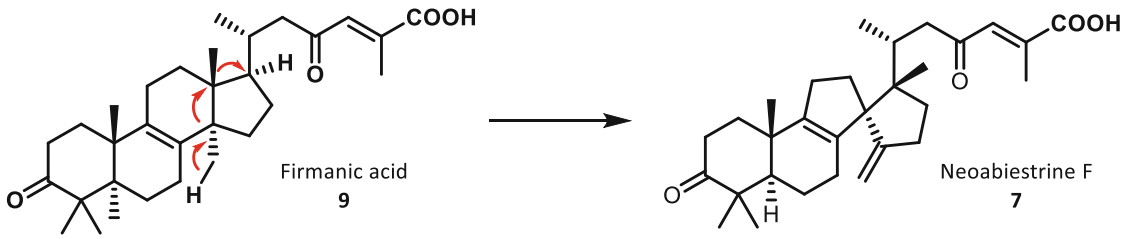

Scheme 2: Firmanic acid and its supposed transformation mechanism to (Z)-Neoabiestrine F [6][7]

The research group around Xiong et. al was also able to identify a number of closely related compounds which can be found in the same plant *Pseudotsuga Forrestii*, namely Forrestiacids C (**10**) and D (**11**) and Forrestiacids E-K (**12-14**, Forrestiacids E, F, G and I not depicted), published in 2022 and 2023, respectively. [7][8]

A selection of those compounds is depicted in Figure 4. All of them are pentaterpenoids derived from a triterpenoid precursor through reaction with an abietane type diterpenoid component. The triterpenoid component always originates from a lanostane type carbon skeleton, either in its regular form or with the C and D ring rearranged to form a spirocycle. They all contain an oxidised sidechain with a ketone on C23, as well as different double bond isomers of α,β-unsaturated carboxylic acids at C26 or C27. [4][7][8]

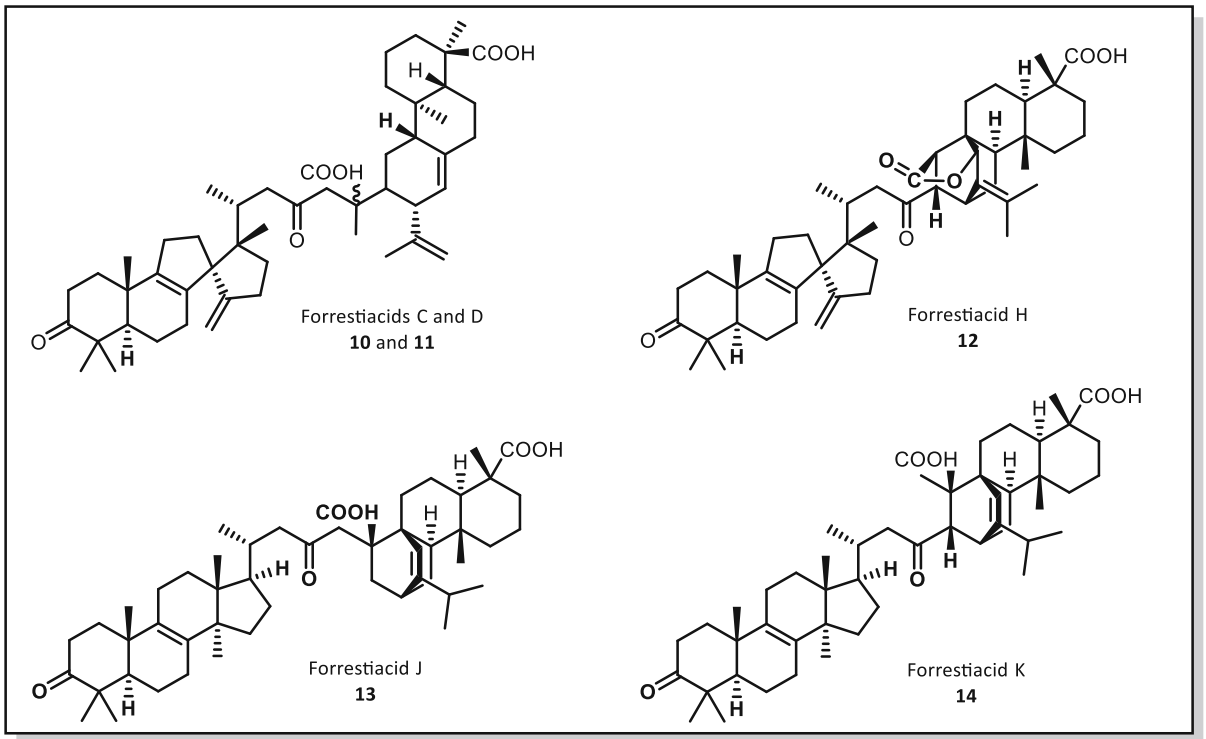

Figure 4: Forrestiacids C, D, H, J and K [7],[8]

Furthermore, Forrestiacids C (**10**) and D (**11**) are not derived from a Diels-Alder reaction, but rather occur as Michael-adducts, where the α,β-unsaturated ketone of the triterpenoid component acts as a Michael-acceptor to react with an abietadiene unit serving as a Michael-donor. [8]

Possible mechanisms forming Forrestiacids are depicted in Scheme 3. It is interesting to note that different double bond isomers of the α,β-unsaturated acid can lead to different cycloaddition products. For example, the (*E*)-configured Neoabiestrine F (**7**) will lead to Forrestiacids A (**5**) and B (**6**) as *endo* and *exo* products, respectively. Firmanic acid would lead to Forrestiacid K (**14**), while its *exo*-double bond analog would form Forrestiacid J (**13**). The depicted transition state T1 refers to formation of Forrestiacid A (**5**) or K (**14**) respectively, whereas T2 refers to formation of Forrestiacid J. Furthermore, possible mechanisms for the Michael-addition of potential abietadiene precursors with the lanostane sidechain are depicted. We suspect that the reaction occurs either through a 1,4-hydride shift in Levopimaric acid (**8**) (Mechanism A) or *via* direct α-H elimination of a neoabietic acid (Mechanism B). [7][8]

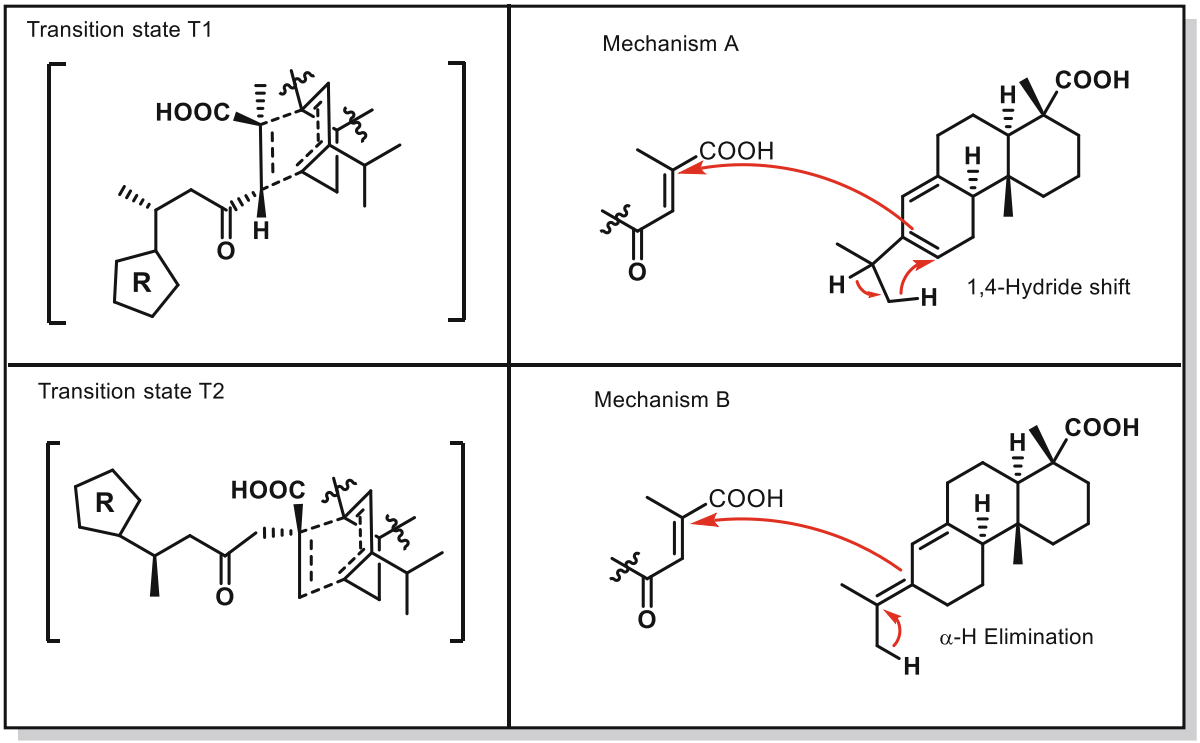

Scheme 1: Possible mechanisms for the Diels-Alder cyclization and Michael-Addition to form Forrestiacids [[]

To conclude, Forrestiacids form a family of complex, structurally similar naturally occurring pentaterpenoids. They can be thought of as heterodimeric adducts. One component is an abietane-type diterpene, for example Levopimaric acid (**8**)**,** which acts as the diene component in a Diels-Alder reaction or as the donor in a Michael reaction. The other component is a lanostane-derived triterpenoid, with an oxidized sidechain containing a double-bond with electron-withdrawing groups, subsequently acting as the complementary dienophile or Michael-acceptor. Their structural similarity to the natural lanosterol potentially allows for synthesis routes from common precursors, making Forrestiacids interesting targets for total synthesis. [4][7][8]

2 Goal of this work

The following Scheme 4 shows the retrosynthetic analysis for Forrestiacid B. The first apparent disconnection is a *retro*-Diels-Alder reaction, giving the two formerly isolated and characterised natural products Levopimaric Acid (**8**) [9] and Z-Neoabiestrine F (**7**) [6]. The former is a commercially available, though expensive, diene, therefore it needs not necessarily be synthesized and will only be of interest for future attempts on the Diels-Alder cycloaddition. [10] The dienophile component Z-Neoabiestrine F (**7**) serves as key intermediate target with well-reported data to identify stereochemistry of products *en route* to Forrestiacids. [6]

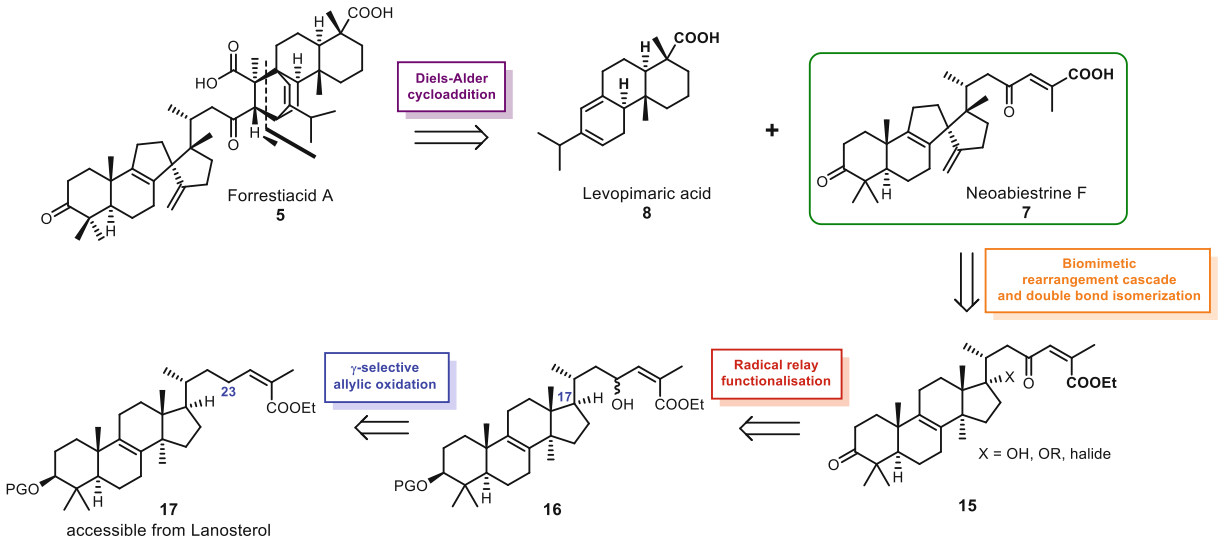

Scheme 2: Retrosynthetic analysis of Forrestiacid B

Neoabiestrine F (**7**) can in turn be derived from an oxidized lanostane type precursor, similar to the proposed biosynthesis (see Scheme 5). [4] The spirocyclization comes about via Wagner-Meerwein rearrangement of the C18 methyl group to the C17 position, rearrangement of the C and D ring to form the spirocycle and elimination of a proton from the C30 methyl group forming an exo double bond with C15. For this to occur, the C17 position must be activated. In nature this most likely happens enzymatically, either through direct abstraction of hydrogen or an activated intermediate **18**. Another synthetic option is to substitute the hydrogen with a suitable leaving group like an activated alcohol derivative or a (pseudo)-halogen. This is indeed a rather challenging feat as one must find a way to selectively target the remote and unreactive C17-H bond.

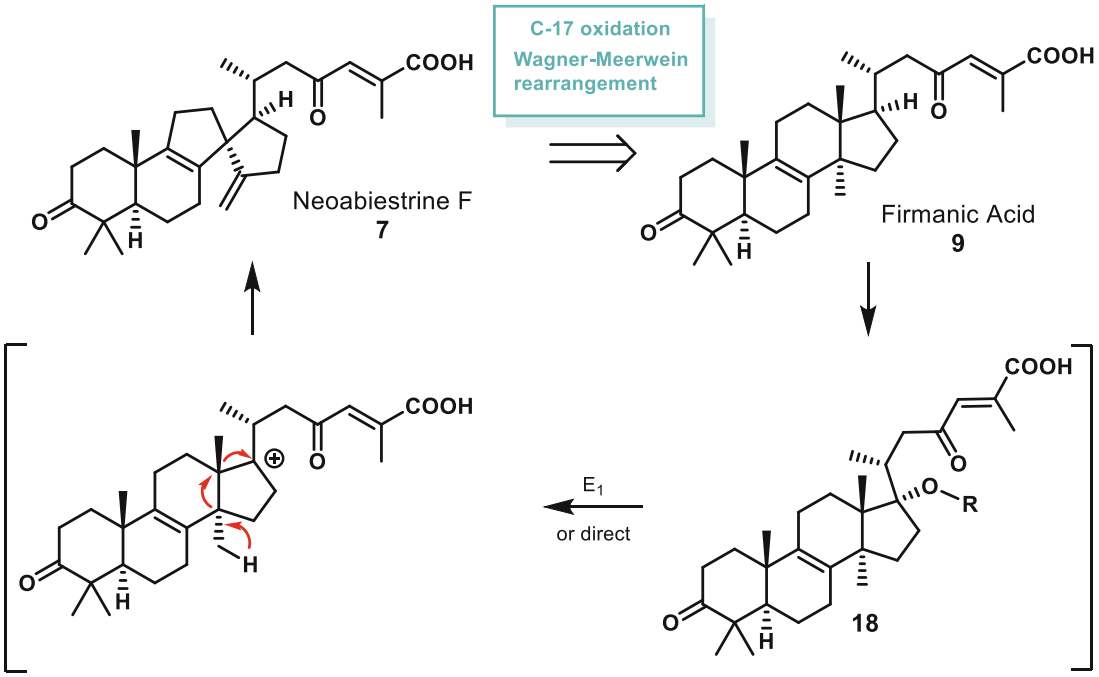

Scheme 3: Proposed mechanism for the rearrangement of firmanic acid to form Neoabiestrine F [4]

The primary strategy to address this issue in this project is to utilize a 1,5-Hydrogen Atom Transfer (HAT) reaction. As there are no reactive groups near our target position, it is hard to activate the C-H bond as well as to differentiate from the chemically similar environment in an intermolecular manner. A radical reaction delivers the high-energy pathway necessary to make the abstraction of hydrogen possible while the 6-membered transition state should ensure regioselectivity. To create an oxygen-centred radical from an alcohol there are a number of different reagents that are able to form a labile O-heteroatom bond, for example PIDA, lead tetraacetate or hypochloric acid. The O-heteroatom bond can then be cleaved (e.g. *via* irradiation) creating a radical on the oxygen which can then trigger the 1,5-HAT forming a tertiary alkyl radical at C17. This should finally recombine, for example with elemental iodine or NBS, determining the substituent of the product **15** at C17. [11]

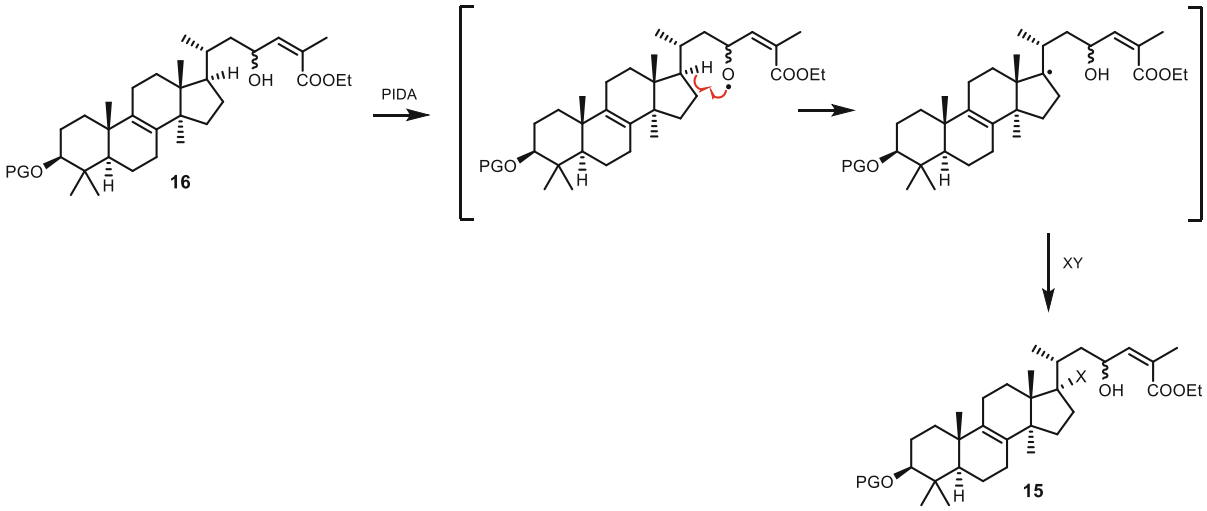

Scheme 4: Rationale for the 1,5-HAT mediated by an oxygen radical [11]

Of course, this approach can encounter many difficulties. The depicted precursor has a neighbouring π-system which could interfere. To prevent a possible 1,5- HAT with the more reactive allylic methyl group, it is chosen to first test this reaction with a derivative in the (Z)-configuration and perform isomerization of the double bond at a later stage.

To evaluate these direct C-17 functionalizations with an elaborated sidechain, one must first find a practical route starting from lanosterol by strategic oxidation and functionalization of the sidechain. The goal of this work therefore consists in the synthesis of a γ-hydroxy-α,β-unsaturated intermediate (**16**) from Lanosterol (**1**).

3 State of the art

3.1 Rearrangements of the lanosterol skeleton

Compton and Harris were able to achieve the desired spirocyclization on lanosterol type compound **19** using Shi's Zn-carbenoid. Creating a carbocation on C13 led to attack of a neighbouring oxygen atom and a Wagner-Meerwein rearrangement of the C and D ring, delivering product **21** after hydrolysis. This required for a starting material with a 13,14-double bond and a hydroxy-group in (*S*)-configuration at C7. [12]

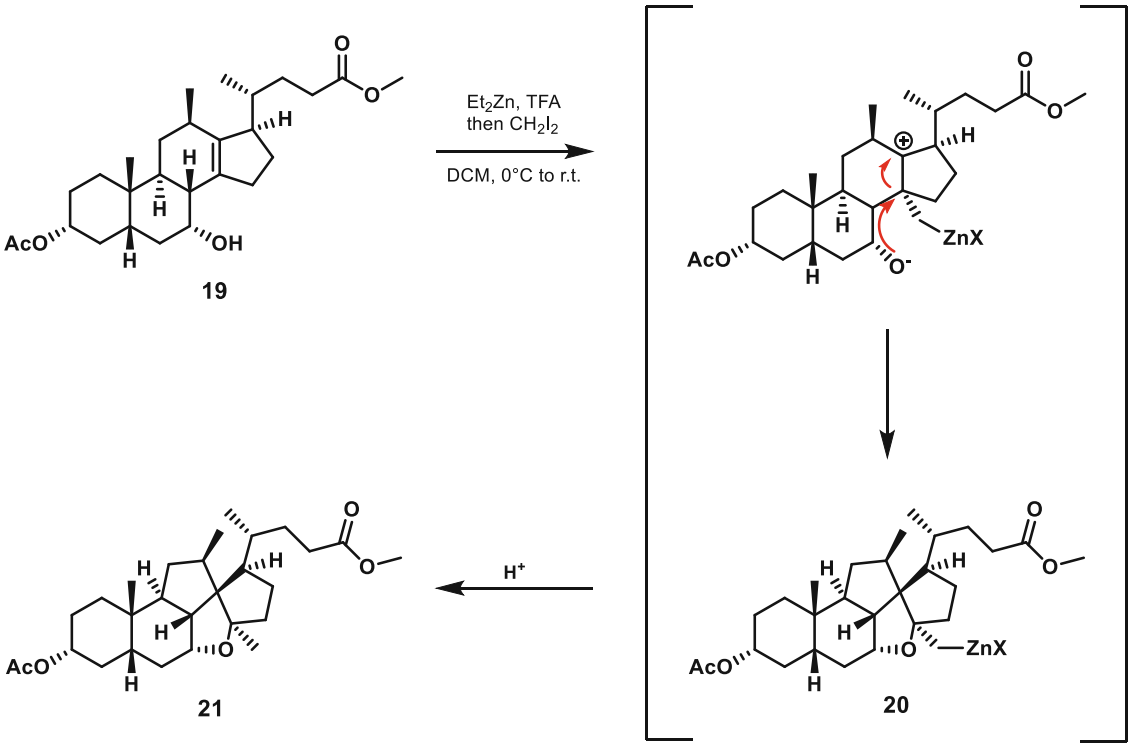

Scheme 5: C/D-Ring spirocyclization of a lanosterol derivative via the Shi-Zn carbenoid accomplished by Compton and Harris [12]

The total synthesis of Spirochensilide A by Wu and Deng also used Lanosterol as the starting material and contains some potentially useful reactions to apply to our synthesis. It starts with ozonolysis, which leads to cleavage of the sidechain double bond to the corresponding aldehyde and to epoxidation of the 8,9-double bond. The resulting aldehyde is then transformed into trifluoromethyl ketone **23**. This serves as precursor for oxidation of C17 to form alcohol **25**, which is further transformed into the corresponding C16,C17-epoxide **26**. Starting from this, a sequence of Wagner-Meerwein rearrangements followed by a Meinwald rearrangement is triggered under Lewis-acid activation, resulting in the rearranged B and C ring spirocycle of **28**. This is followed by a series of modifications on the sidechain and, finally, a photoinduced spiroketalization, resulting in Spirochensilide A (**31**) as the final product. [13]

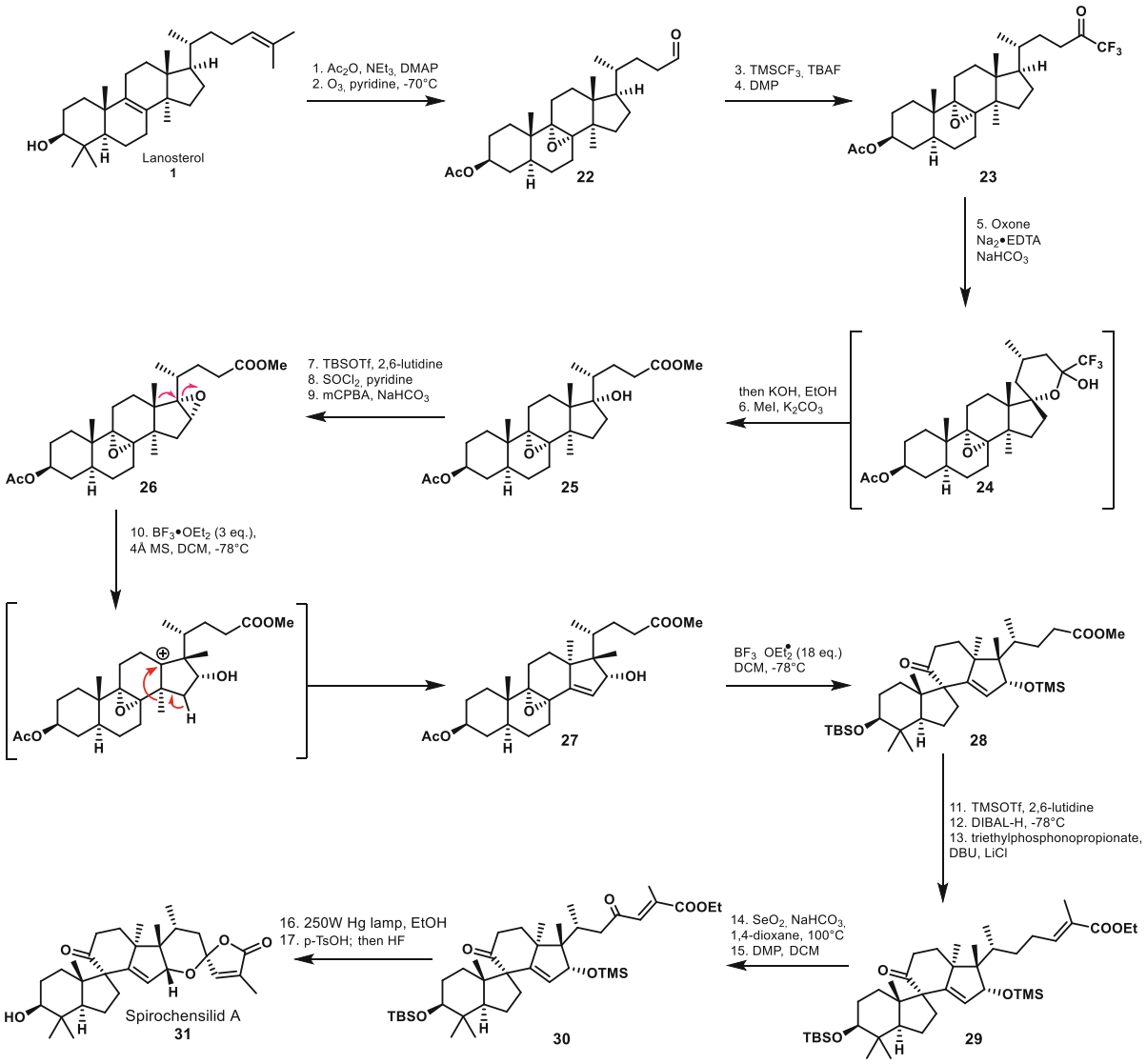

Scheme 6: Reaction scheme for the total synthesis of Spirochensilide A by Wu and Deng [13]

Most noteworthy for our avenue is the C17-activation using Oxone on a trifluoromethyl ketone, leading to formation of lactol **24**, which is then hydrolysed, leading to substitution at C17 with a hydroxyl-group in a stereoselective manner forming compound **25** after methylation. Also worth noting are the late-stage sidechain oxidations leading to compound **30**. [13]

3.2 1,5-HAT reactions

An early example by Walling and Padma dating back to 1961 is the synthesis of δ-chlorohydrins from the corresponding hypochlorites *via* photolytic cleavage and subsequent 1,5-HAT, where the chloride radical formed in the cleavage then acts as scavenger. However, a severe drawback is the need to isolate the often unstable primary and secondary alkyl hypochlorites before photolysis. Furthermore, no examples of tertiary hydrogen abstraction were reported. [11][14]

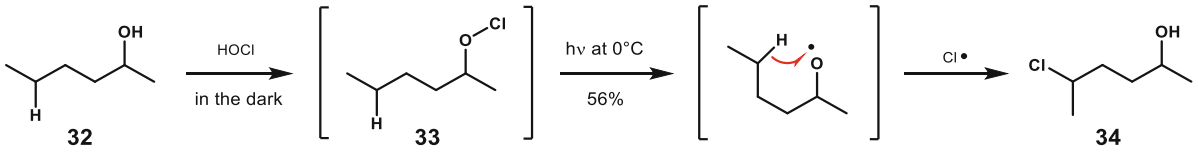

Scheme 7: Synthesis of a Chlorohydrin via 1,5-HAT from an alkyl hypochlorite [11]

Following milder conditions were developed in the form of using hypoiodite species, which can be photolyzed without the need for isolation. One method involves the use of PIDA to generate hypoiodite species *in-situ*. After ligand exchange, this forms a hypoiodite-O-alkyl intermediate which can undergo homolytic cleavage under irradiation with visible light to form an oxygen-centred radical. This can then induce the 1,5-HAT, reforming the alcohol and creating an alkyl radical, which is then scavenged by iodine. The alcohol can then again be transformed into a hypoiodite, allowing for radical cyclization to give tetrahydrofuran derivatives. The mechanism depicted in Scheme 10 is simplified and does not include further reaction pathways like additional 1,5-HAT leading to further side products. [11]

Another reagent for *in-situ* formation of hypoiodite species is lead tetraacetate. This approach can also allow for isolation of iodohydrins, if reaction times are short or substoichiometric amounts of reagents are used. [11][15]

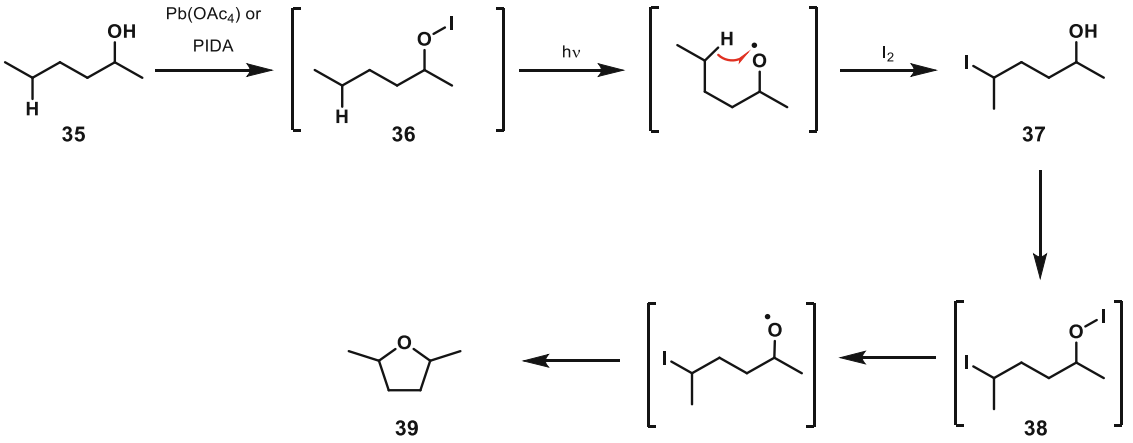

Scheme 8: 1,5-HAT using lead tetraacetate [11]

This methodology has been successfully implemented in the total synthesis of natural products. One example of this is the total synthesis (-)-Jiadifenoxolane (**42**) by Maimone and coworkers, where applying the hypoiodite reaction to (+)-Cedrol (**40**) led to formation of a tetrahydrofuran ring, which was then opened by addition of acetic anhydride and phosphoric acid, giving the acetylated product **41** in one step. [16]

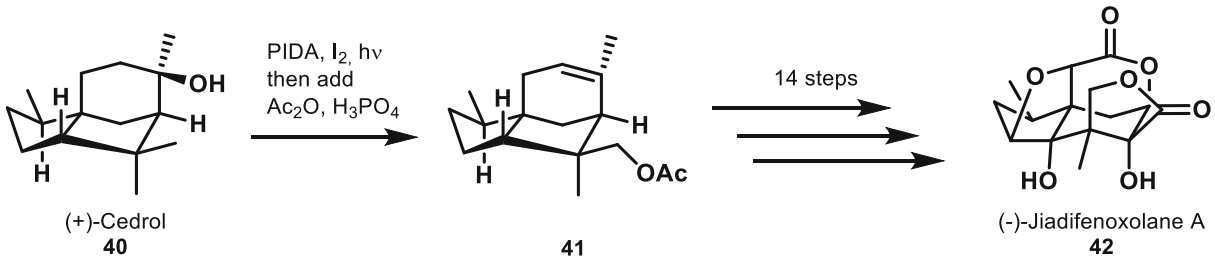

Scheme 9: Total synthesis of (-)-Jiadifenoxolane A applying the hypoiodite reaction [16]

A more modern approach is found in the photoinduced remote C(sp^3)-H cyanation vinyl radical 1,5-HAT methodology developed by Guo and Xia. It makes use of an Iridium photoredox catalyst under irradiation with blue LEDs at 450 nm to induce homolytic decarboxylative cleavage of phthalimido esters **43** followed by addition of a substituted alkyne **44**. This leads to formation of an alkene radical which then triggers the 1,5-HAT. Finally, using TMSCN and CuI as catalyst leads to cyanation of the radical position. Additionally, the alkyne must be substituted with an electron-withdrawing group (EWG) and an aryl group or EWG. Nonetheless, it can serve as a model for future explorations of suited 1,5-HAT conditions. [17]

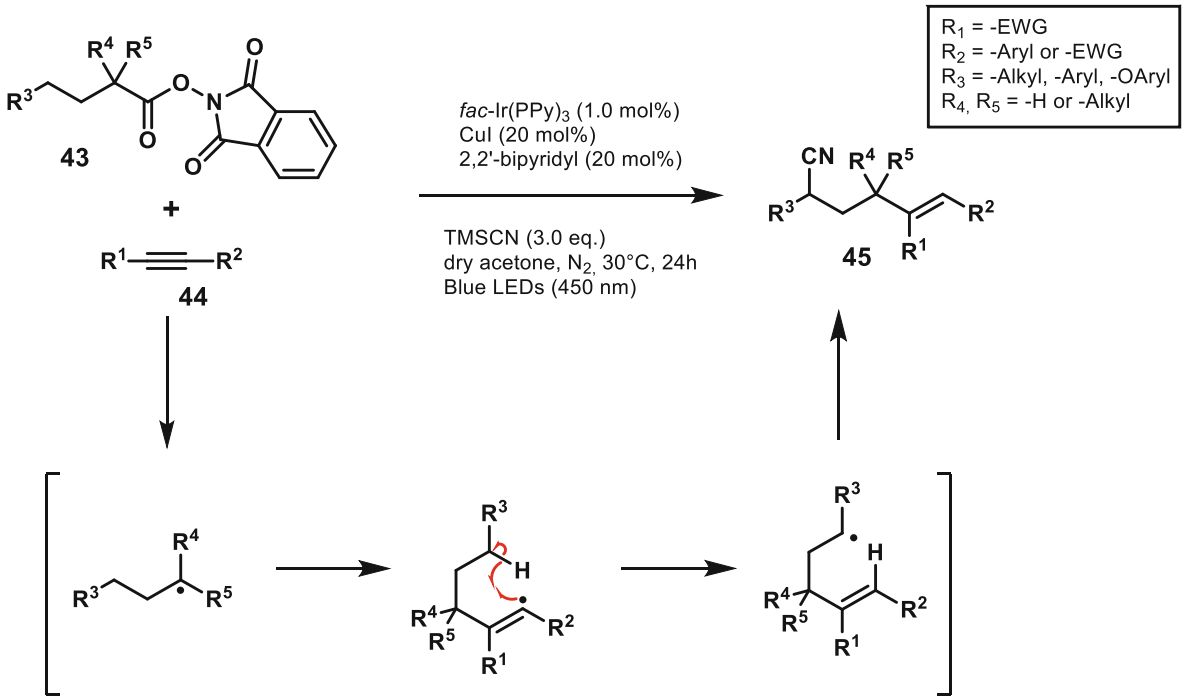

Scheme 10: Photoinduced Remote C(sp^3)-H Cyanation Vinyl Radical 1,5-HAT [17]

4 Synthetic Work

4.1 First Steps – Protection of the C-3 and establishing the reactivity of the sidechain under Riley oxidation conditions

The synthesis starts from commercially available lanosterol (**1**) which is commonly sold as a mixture containing Agnosterol (**46**) and the 24,25-dihydro derivatives of Lanosterol **47** and Agnosterol **48** (figure 5) where lanosterol constitutes the main component of around 55%. A few words concerning the reactivity and analysis of the mixture, the cyclic diene compounds can be identified, and their content approximated by two distinct olefinic peaks in the ^{1}H-NMR adding up to around 4% (24,25-dihydro-)Agnosterol. Similarly, the sidechain olefin content can be approximated by comparing the integrals of the clear-cut signals of the C3-H (which all the compounds share) and the olefinic C24-H. [18][19]

Pertaining to the reactivity it should be mentioned that all compounds contain a hydroxyl group at the C3 and should therefore react equally when this position is targeted, which will be the starting point of our reaction sequence. Subsequently, the sidechain olefin will be of interest and therefore only the 24,25-alkene compounds **1** and **46** should react, leaving behind the dihydroderivatives **47** and **48** as unreacted starting material.

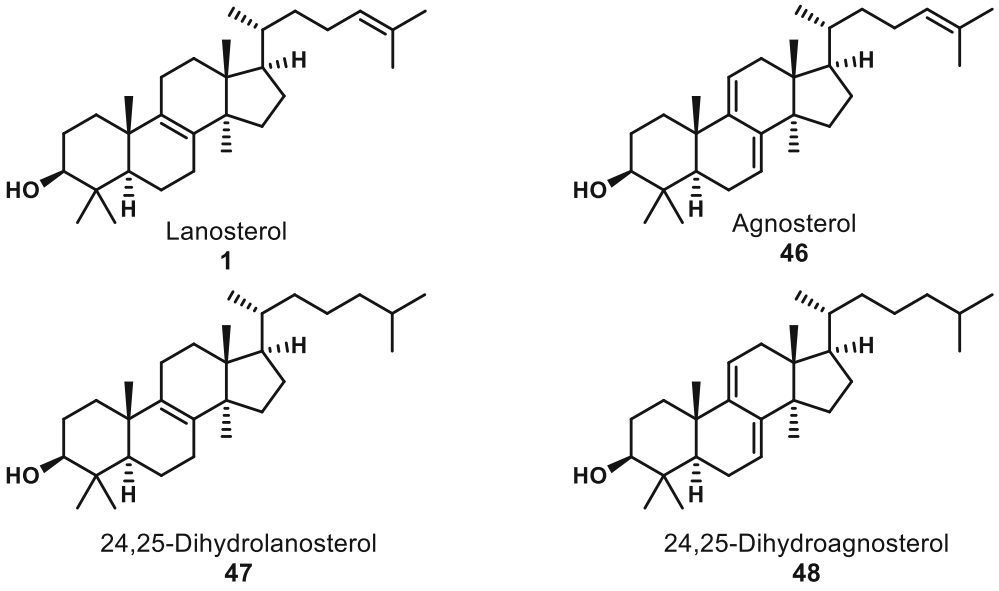

Figure 5 Composition of the commercial product lanosterol

In designing the forward synthesis, there is a broad choice of different synthetic routes, concerning the type of transformations and the order in which they are applied (see Scheme 13). It can start by either oxidative cleavage of the sidechain double bond of **49** resulting in carboxylic acid **50**. Alternatively, either by redox neutral-cleavage of **49** or reduction of **50**, aldehyde **52** can be obtained. From there on the synthesis can procced *via* α-oxidation followed by Still-Gennari olefination or begin with the Still-Gennari olefination followed by a γ-oxidation to form target compound **16**. Another approach starts by Riley oxidation of the allylic C26 position to form allylic aldehyde **51**, which then must be further oxidized and isomerized to yield intermediate **17** for γ-oxidation.

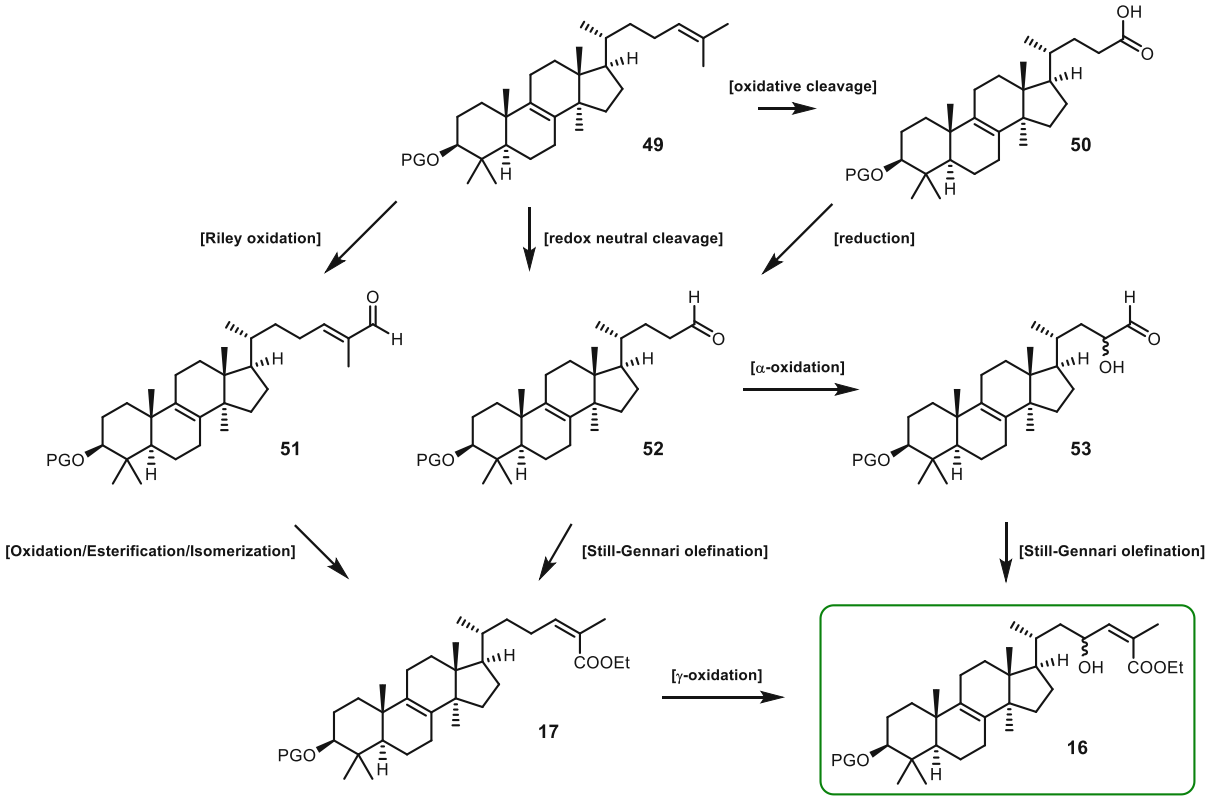

Scheme 11: Variety of proposed forward syntheses

As the C3-alcohol is the only potentially intervening functionality, it should be protected first. Consequently, an acetyl group was introduced using acetic anhydride, triethyl amine and DMAP. This reaction yielded the 3-OAc protected compound **54** in almost quantitative amounts.

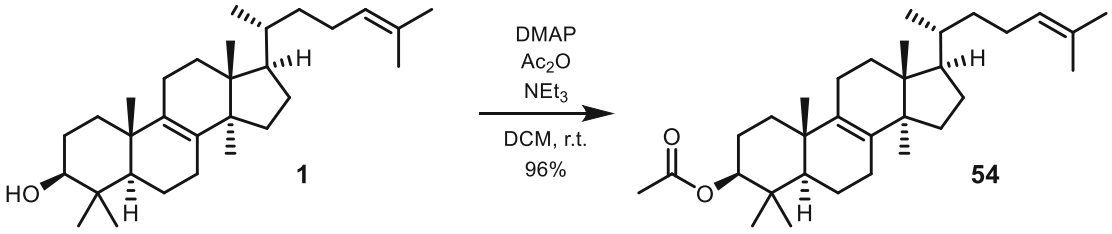

Scheme 12: Acetyl protection of the free alcohol

Protection with a TBS-group using TBSOTf and lutidine was also successful, giving a moderate yield of **55** but it turned out that protecting the 3-position with a TBS-group leads to solubility issues in the highly polar solvents needed for most of the established transformations later in the synthesis, so this approach was discarded quickly.

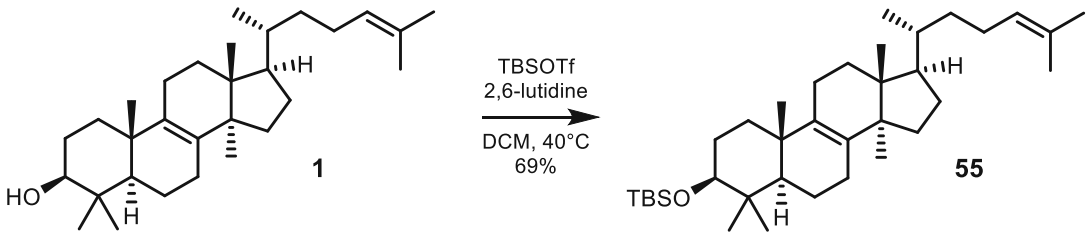

Scheme 13: TBS-protection of the free alcohol

In the beginning stages, the direct oxidation of the allylic methyl groups was explored. The Riley oxidation is known for its ability to selectively oxidize allylic methyl groups, with preference for (*E*)-configured products and attack at the less sterically hindered side. The mechanism illustrated below (Scheme 14) demonstrates how, in the transition state a five-membered ring is formed, where both the methyl group and R are in pseudoequatorial position resulting in both of them being on the same side of the double bond, thus ensuing the (*E*)-configuration of the resulting α,β-unsaturated aldehyde or allylic alcohol. Additionally, mechanisms are suggested by us of how employing either a catalytic amount of SeO_2 and tBuOOH as reoxidant at room temperature or a stoichiometric amount of SeO_2 at elevated temperature can lead to distinct pathways. These pathways lead to formation of either an alcohol or aldehyde type product, as also depicted. [20]

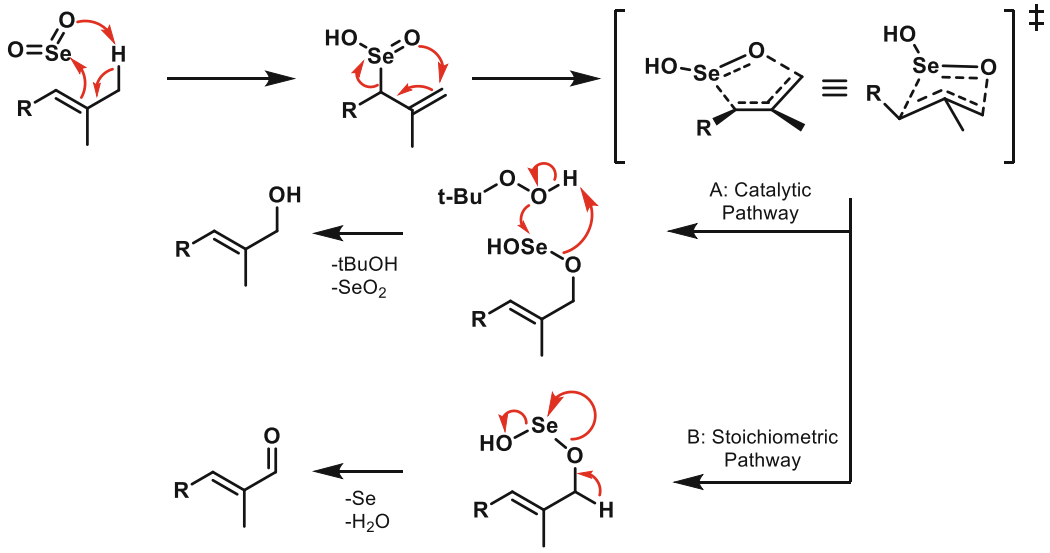

Scheme 14: Mechanism of the Riley oxidation

A small screening was done, implementing slightly different conditions for the catalytic Riley oxidation as shown below. All trials yielded the expected (*E*)-allylic alcohol product **56**, however, the yields were unsatisfactory.

Table 1: Condition screening for catalytic Riley oxidation

SeO_2	tBuOOH	Additive	Solvent	yield
0.2 eq.	4 eq.	-	THF	10%
0.2 eq.	4 eq.	-	DCM	14%
0.1 eq.	4 eq.	0.1 eq. salicylic acid	DCM	20%

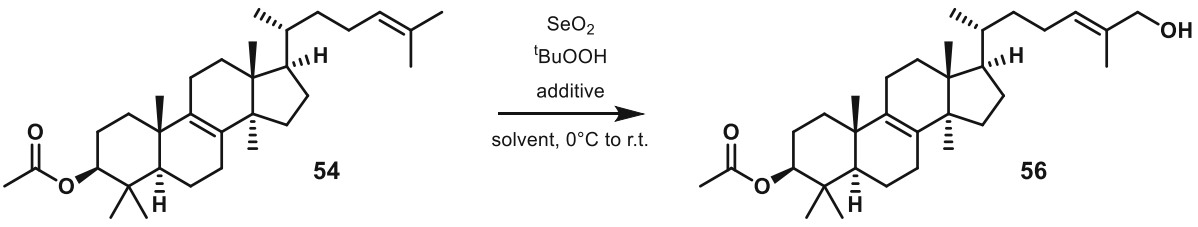

Scheme 15: Riley oxidation using catalytic amounts of SeO_2

Implementation of stoichiometric amounts of selenium dioxide directly yields the (*E*)-α,β-unsaturated aldehyde product **57** with moderate yields. As this is quite an early step in the total synthesis those were not satisfactory, especially regarding the early use of highly toxic selenium dioxide, also considering a future scale-up. Therefore, no further exploration of this path has been undertaken to date.

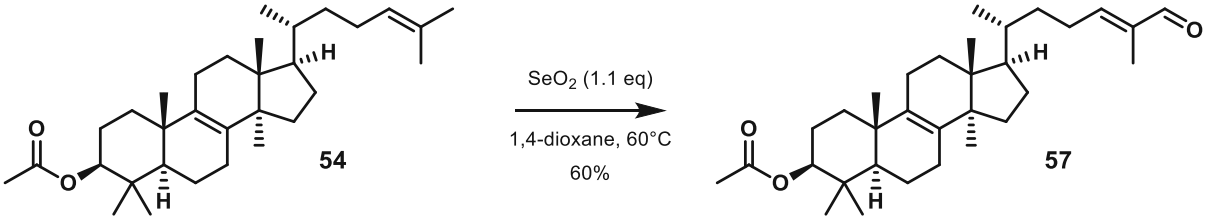

Scheme 16: Riley oxidation using stoichiometric amounts of SeO_2

4.2 First breakthrough – Development and optimization of conditions for cleavage of the sidechain olefinic bond to the corresponding aldehyde

Several different methodologies were examined for the oxidation and subsequent cleavage of the side chain double bond. While many methods were able to discriminate between the more accessible sidechain olefin and the 8,9-tetrasubstituted alkene, ozonolysis led to formation of an epoxide in the 8,9-position to a significant extent. Application of catalytic osmium tetroxide and NMO as reoxidant in one pot with sodium periodate resulted in a mixture of different products, none of which was the desired aldehyde.

One-pot dihydroxylation and diol-cleavage with potassium permanganate and sodium periodate resulted in oxidative cleavage of the sidechain double bond, yielding the corresponding carboxylic acid **58**. Due to the oxidative properties of permanganate, however, the reaction does not stop there, and the carboxylic acid thus needs to be reduced subsequently.

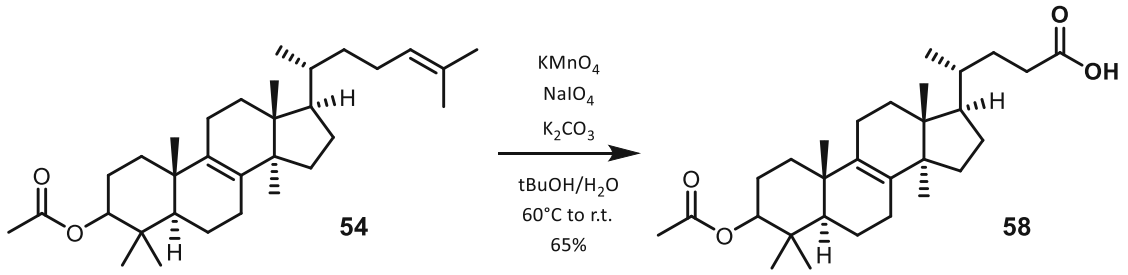

Scheme 17: One pot dihydroxylation of sidechain double bond and subsequent oxidative cleavage to carboxylic acid

The carboxylic acid was accordingly transformed with oxalyl chloride into the corresponding acyl chloride **59**. This intermediate was not isolated but directly subjected to reduction.

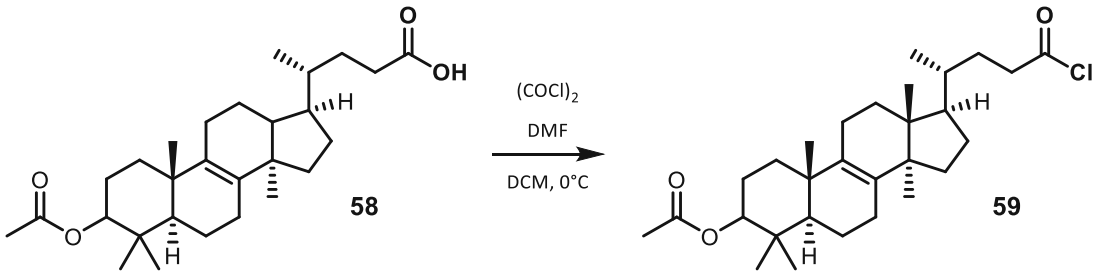

Scheme 18: Formation of the acyl chloride

Use of lithium tri-tert-butoxyaluminum hydride as a mild reducing agent for the acyl chloride **59** at low temperature resulted in over reduction to the alcohol, rather than the desired aldehyde **60**. Conclusively this laborious multi-step approach was discarded in favour of finding a way for redox-neutral diol-cleavage.

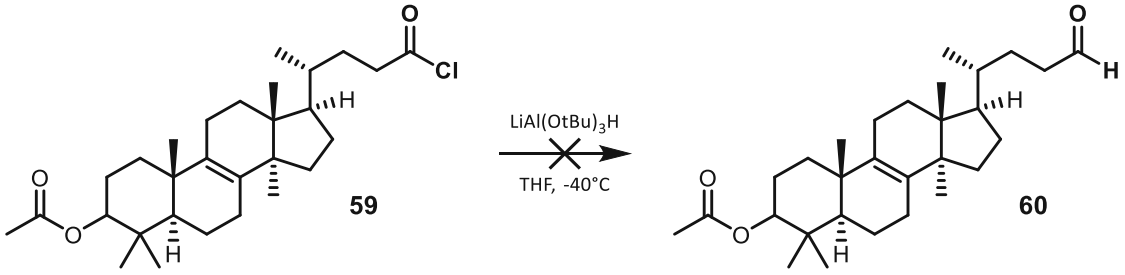

Scheme 19: Failed attempt at reducing the acyl chloride to an aldehyde

In reference to a study on the purification of lanosterol, a two-step, one pot procedure for dihydroxylation was adapted, allowing for isolation of a diastereomeric mixture of 3-OAc-lanostane-24,25-diols **61A/B**. The original workup consisted of precipitating the product by addition of water and subsequent vacuum filtration. This, however, worked only one time. Repeated experiments lead to significant clogging of the glass-sintered filter, rendering this workup method inapplicable. Instead, the solvents had to be removed in a time-consuming manner by evaporation *in vacuo*. The mixture of diols could then be isolated using flash chromatography. [21]

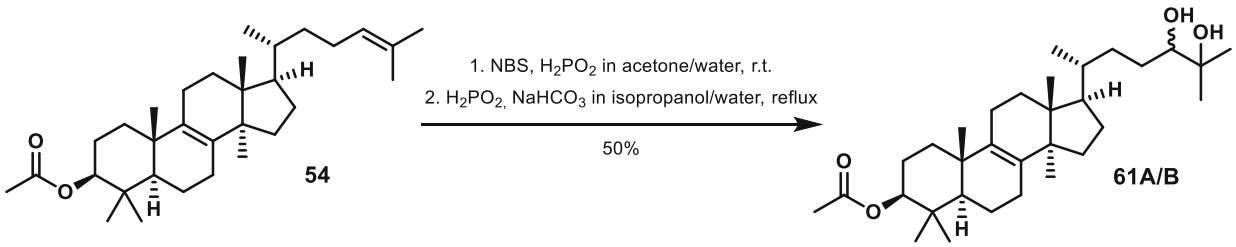

Scheme 20: Dihydroxylation of the sidechain double bond

Now, a suitable procedure for cleavage of the diastereomeric diols **61A/B** to form aldehyde **60** had to be found. Applying PIDA as reagent for the diol cleavage led to unsatisfactorily low yields. Using lead tetraacetate instead resulted in higher yields of around 73%, but still needed chromatographic purification.

The diols were then submitted to cleavage using sodium periodate, yielding a clean aldehyde product in high yields with no further purification necessary, provided that the starting materials were reasonably pure.

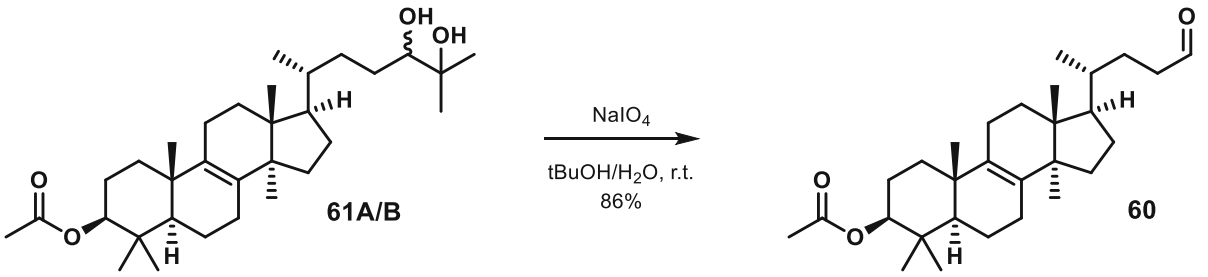

Scheme 21: Cleavage of the diol yielding an aldehyde

Because of the cumbersome workup yet another approach was tested. A literature protocol for epoxidation of the lanosterol sidechain double bond was applied, giving diastereomeric mixtures of epoxides **62A/B** in higher yields than the dihydroxylation with a more facile workup. [22]

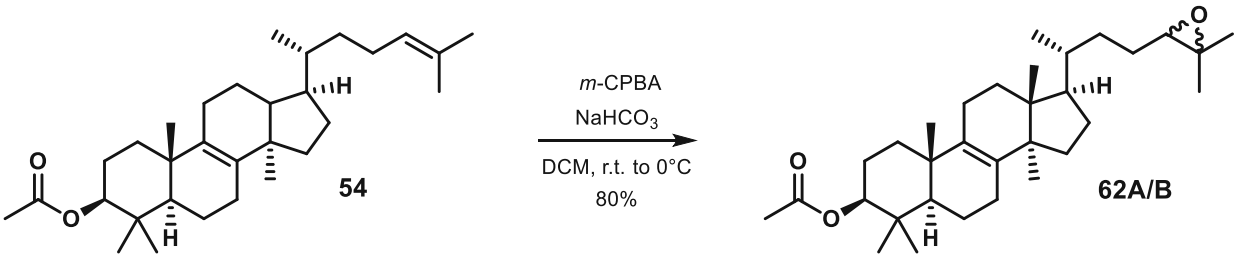

Scheme 22: Epoxidation of the sidechain double bond

In a similar manner to the diol, the epoxide can be cleaved using periodic acid and sodium periodate. Again, a highly pure substrate yields almost quantitative amounts of high purity aldehyde.

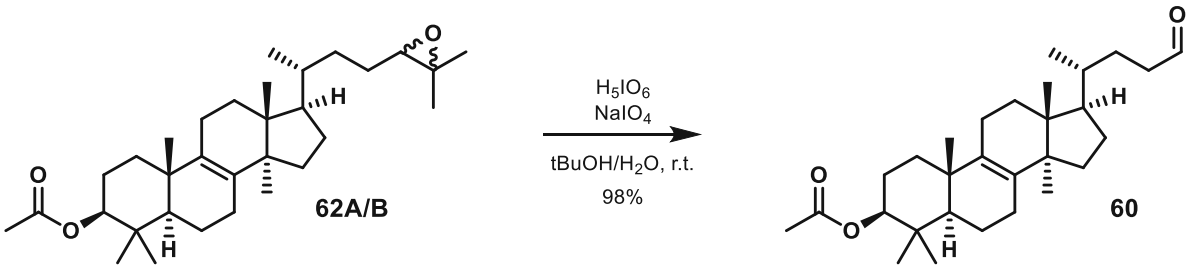

Scheme 23: Epoxide opening and cleavage

This most satisfying approach in terms of yields and ease of application now constitutes our standard procedure for synthesizing the required aldehyde.

4.3 Attempts at α-oxidation of the aldehyde

The next field of exploration was the possibility of oxidizing the aldehyde in α-position to create a precursor for an oxygen-centred radical. α-Oxyacylation with Propanoic acid using an in-situ generated (hypo-)iodite catalyst led to no formation of the desired product **63**. [23]

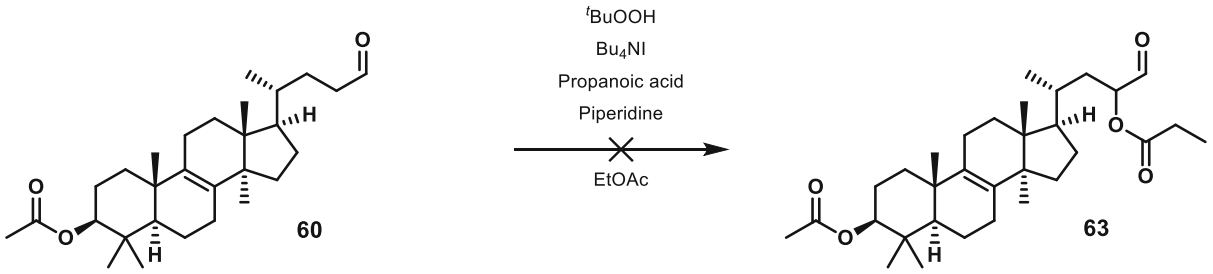

Scheme 24: α-Oxyacylation of the aldehyde

Another interesting protocol explored was the stereoselective direct Proline-catalysed α-aminoxylation with Nitrosobenzene. Unfortunately, we were again unable to identify the desired product **64**. [24]

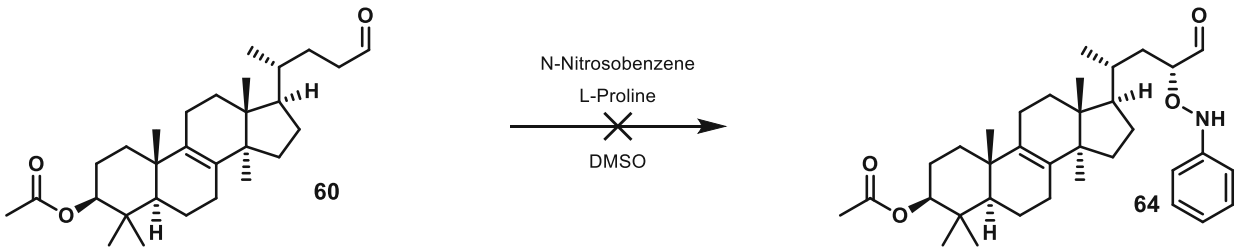

Scheme 25: α-Hydroxylation of the aldehyde

The third approach was a photocatalytic 1C-dehomologation using $Ru(bpy)_3Cl_2$ as photocatalyst and oxygen as the terminal oxidant. This reaction did indeed yield an inseparable mixture of aldehydes of different chain length. Given that the original publication was designed for the synthesis of ketones from aldehydes with a tertiary carbon in α-position, this result was not surprising. [25]

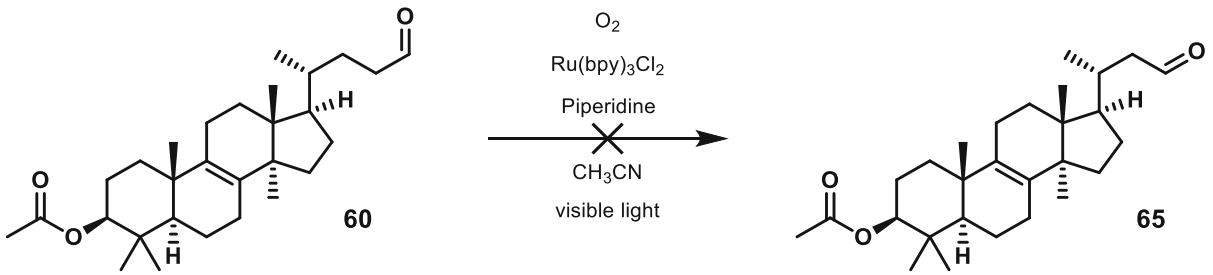

Scheme 26: Oxidative Cleavage/Dehomologation of the aldehyde

With these three approaches the repertoire of possible transformations to attempt was exhausted. Therefore, the next endeavour was to reconstruct the sidechain while simultaneously introducing an α,β-unsaturated ester.

4.4 Evaluation and optimization of HWE and Still-Gennari conditions

Armed with the critical aldehyde, it became possible to explore ways of synthesizing the α,β-unsaturated C26 and C27-carboxylic acid ester derivatives of lanosterol. The possible (*E*)- and (*Z*)- isomers could both act as possible precursors for various Forrestiacids, so it was deemed useful to find approaches for each.

Initially, we approached the synthesis of the (*E*)-α,β-unsaturated-ester **67** using the stabilized phosphonester triethylphosphonopropionate **66** in a Horner-Wadsworth-Emmons (HWE) reaction. The conditions for the HWE were optimized by screening different bases for their yield and (*E*)/(*Z*)-ratio, as detailed below. The best ratio in favour of the (*E*)-isomer was achieved with sodium hydride, yet at a low yield of only 25%. The best option turned out to be NaHMDS with a very good yield of 89% and a 7/1-ratio favouring the desired isomer.

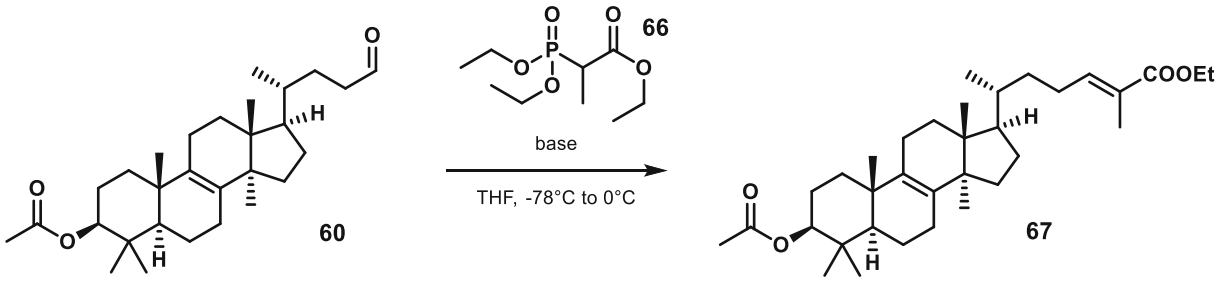

Scheme 27: General reaction scheme for the HWE-reaction

Base	Yield	(*E*)/(*Z*)-ratio
KOtBu	Trace	Not determined
NaH	25%	9:1
KHMDS	64%	2:1
NaHMDS	**89%**	**7:1**

Table 2: Results of the optimization for use of different bases

To obtain the corresponding (*Z*)-isomer the Still-Gennari variant of the HWE reaction was employed. This method uses a phosphonate that is substituted with strongly electron-withdrawing 2,2,2-trifluoroethyl groups which shifts the selectivity toward the (*Z*)-isomer. The necessary reagent was readily prepared from the commercially available reagent of the previous reaction, in analogy to the literature. [26]

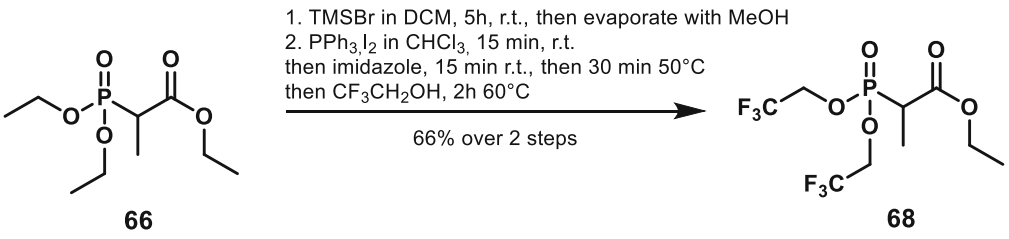

Scheme 28: Synthesis of the Still-Gennari reagent

The protocol for the synthesis of the Still-Gennari reagent **68** involved synthesizing the free phosphonic acid followed by substitution under Garegg-Samuelsson conditions in a two-

step, one-pot procedure. A facile workup by vacuum distillation allowed for a quick and easy preparation on a multi-gram scale. [26]

The Still-Gennari reaction was conducted in analogy to the HWE reaction using the modified phosphonate **68**, KHMDS as base and the corresponding crown ether [18]-crown-6 as additive. Satisfactorily, this led to exclusive formation of the (*Z*)-α,β-unsaturated ester **69** in very good yields, up to a one-gram scale.

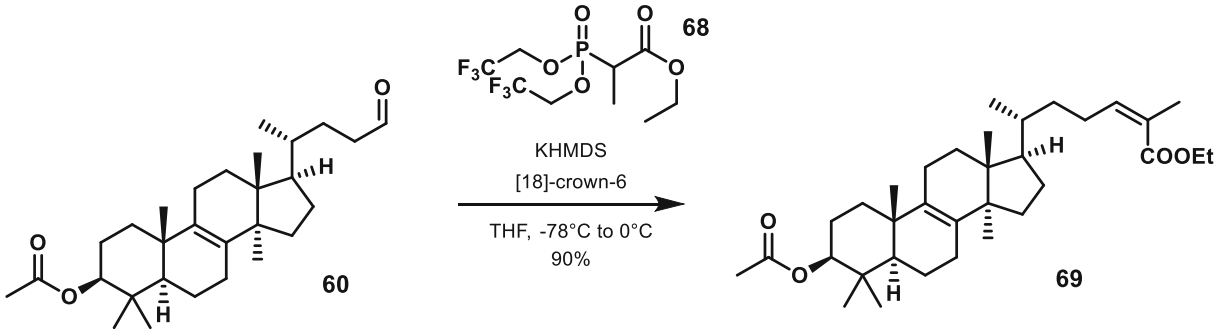

Scheme 29: Reaction scheme for the Still-Gennari reaction

Now that both α,β-unsaturated esters can be selectively synthesized in sufficient yields and scale, the further avenue consists of exploring their γ-hydroxylation.

4.5 Final Steps – γ-hydroxylation and attempted C-17 functionalization

A recently published methodology on visible-light photocatalyzed γ-hydroxylation of α,β-unsaturated ketones was tested on our substrate. The procedure uses Eosin Y as photocatalyst, blue 455 nm LEDs as light source and oxygen as terminal oxidant. It turned out that this procedure is not applicable to α,β-unsaturated ester substrate **69**, so other ways to facilitate γ-hydroxylation were examined. [27]

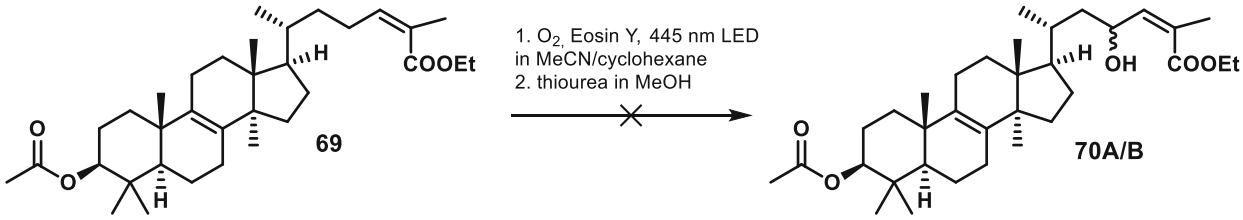

Scheme 30: Attempted photocatalytic γ-hydroxylation

Inspired by the total synthesis of Spirochensilide A by Wu and Deng [13], another idea for achieving this difficult transformation came to mind. Again, the use of selenium dioxide facilitated allylic oxidation (see Scheme 31). Two diastereomeric allylic alcohols at C23 could be isolated in a little over 20% yield each, which are labelled **70A** and **70B** in order of descending R_f (see section 6.2.9). It was possible to separate both diastereomers *via* column chromatography, however, they both showed around 10% of olefinic proton signals in their ^{1}H-NMR spectra, with chemical shifts corresponding to the 7,9(11)-diene structure also found in Agnosterol, indicating that the 7,9(11)-diene analogs of **70A** and **70B** emerge as side products under these conditions.

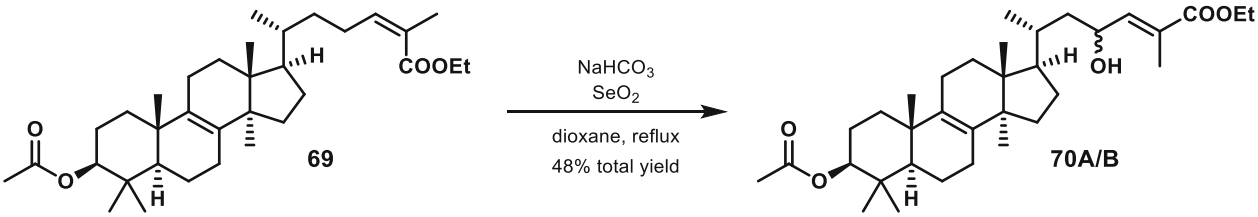

Scheme 31: Successful γ-hydroxylation using selenium dioxide

Additionally, a few milligrams of another side product could be isolated. The comparison of its ^{1}H-NMR spectrum with the product of Dess-Martin oxidation of the alcohol mixture **70A/B** suggests that it could be C23-ketone product **71** (*vide infra)*. This further led to reconsideration of the double bond configuration of allylic alcohols **70A/B**. They were finally assigned in (*E*)-configuration by comparing the chemical shifts of the olefinic protons with those reported for structurally very similar intermediates in the total synthesis of Spirochensilide A. For comparison, the ^{1}H-NMR spectra of **70A/B** are depicted in Figure 6, along with an analysis of the olefin signals in comparison to reported literature. It shows, that the chemical shifts are basically identical, which underpins the assignment for **70A/B** as diastereomeric allylic alcohols in (*E*)-configuration, and not the (*Z*)-configuration expected and desired for testing the 1,5-HAT. [13]

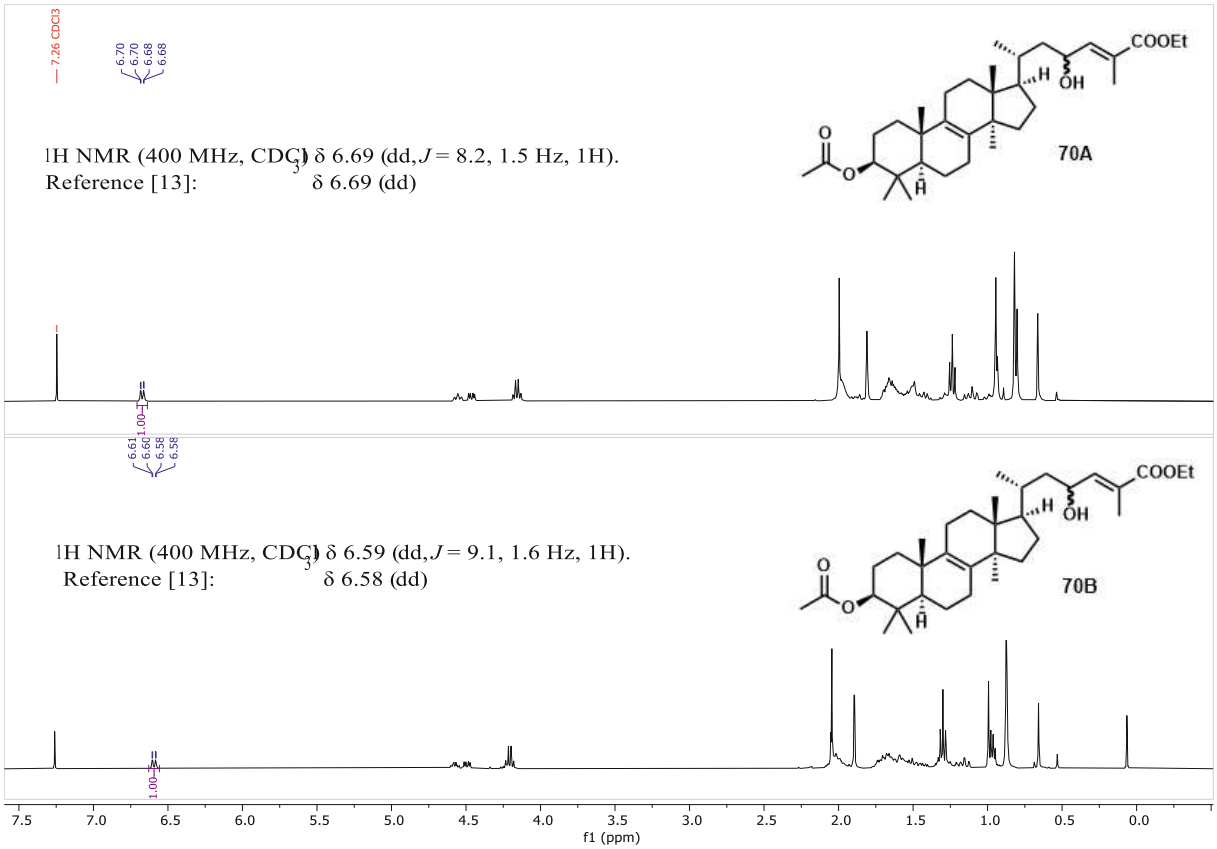

Figure 6: 1-H NMR spectra of the two allylic alcohols showing the chemical shifts of the olefinic protons

A small sample of the mixture of diastereomeric alcohols **70A/B** was subjected to Dess-Martin oxidation, which should result in formation of γ-oxo-α,β-unsaturated ester product **71**. The isolated single product was then subjected to ^{1}H-NMR spectroscopy and compared to the side product of the Riley oxidation.

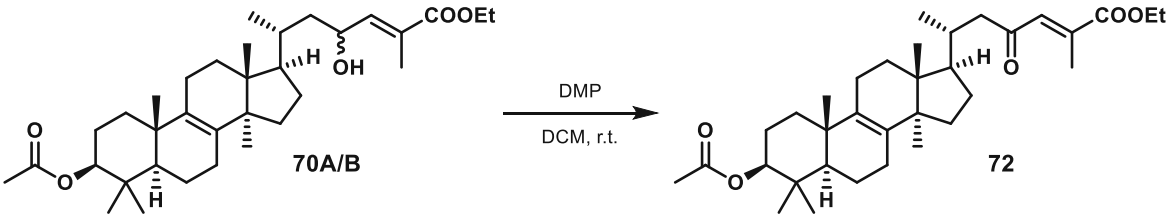

*Scheme 32: Dess-Martin-oxidation of **70A/B***

The following ^{1}H-NMR spectra show selected integrals and chemical shifts, relevant for comparison and assignment of compounds **71** and **72**.

For the side product of the Riley oxidation of **69**, those signals correspond to the following carbon atoms in order from low to high field:

C24-H, C3-H, ethyl-CH_2, two times C22-H, C26-CH_3, ethyl-CH_3, C21-H

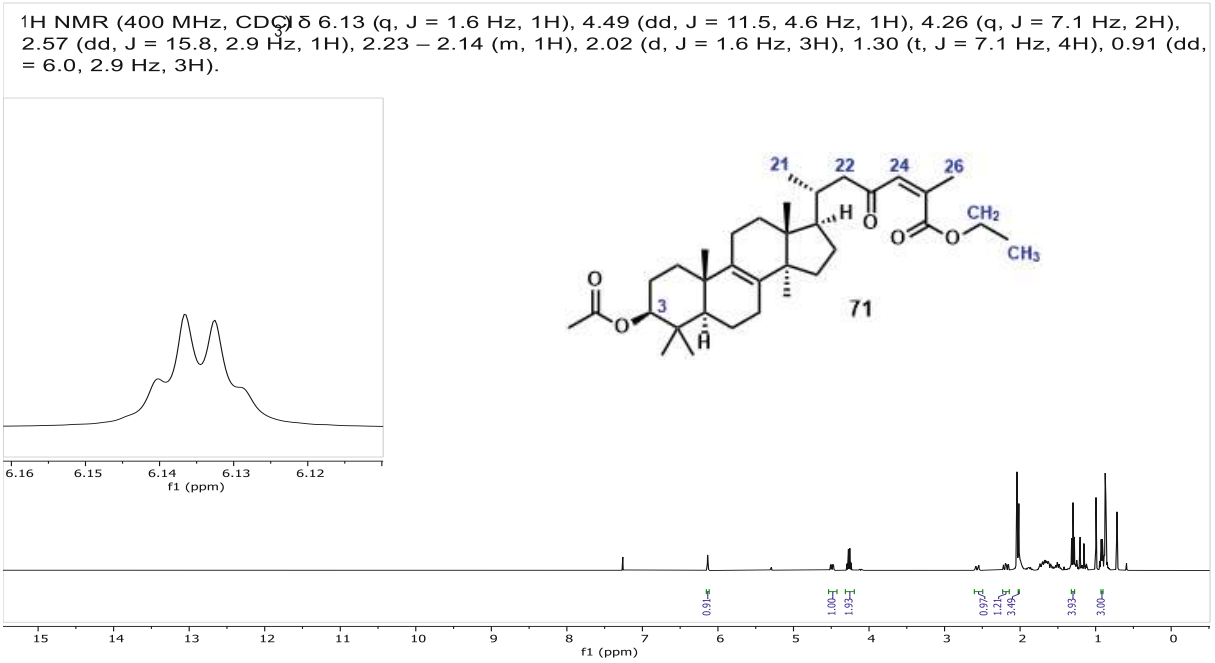

*Figure 7: ^{1}H-NMR of Side Product **71** of Riley oxidation of **69***

For the product **72** of the Dess-Martin oxidation, those signals correspond to the following carbon atoms in order from low to high field:

C24-CH, C3-CH, ethyl-CH_2, two times C22-CH, C27-CH_3, ethyl-CH_3, C21-CH_3

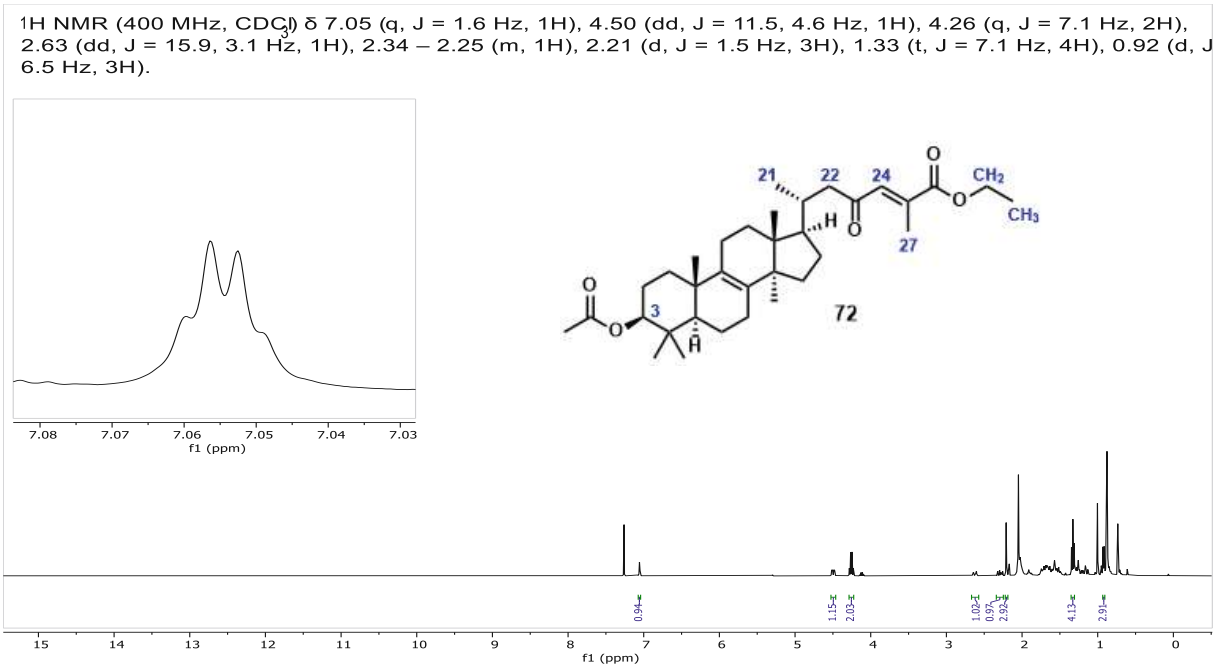

*Figure 8: ^{1}H-NMR of Product **72** of Dess-Martin Oxidation of **70A/B***

The signals of the olefinic protons show almost equal shape and coupling constants for both products but differ almost 1 ppm in shifts. Other than that, the ^{1}H-NMR spectra for both compounds are very similar, both showing isolated signals for the protons on C22 adjacent to the ketone, with similar shifts between 2.14 and 2.63 Hz. The chemical shifts of the olefinic protons coincide well with the shifts reported for very similar natural compounds containing (*E*)- and (*Z*)-configured sidechains, respectively. For comparison, the selected shifts and references are summarized in Table 3 (note that not all the signals can be compared due to the structural differences and lack of assignments for compound **30**). [5][13][28]

Table 3: Comparison of chemical shifts and multiplicities with reported compounds

	(*Z*)-Neoabiestrine methyl ester [28]	Side product of Riley oxidation (**71**)	(*E*)-configured reference compound (**30**) [13]	Product of Dess-Martin oxidation (**72**)
C3-CH	-	4.49 dd	-	4.50 dd
C21-CH_3	0.84 d	0.91 dd	-	0.92 d
C22-CH(1)	2.20 dd	2.14-2.23 m	-	2.25-2.34 m
C22-CH(2)	2.47 m	2.57 dd	-	2.63 dd
C24-CH_3	6.06 q	6.13 q	7.05 d	7.05 q
C26-CH_3	1.98 d	2.02 d	-	-
C27-CH_3	-	-	-	2.21 d
ethyl-CH_2	3.76 s (CH_3)	4.26 q	4.26 q	4.26 q
ethyl-CH_3	-	1.30 t	-	1.33 t

Following are the NOESY spectra for both compounds giving more information to solidify the assumed configuration.

The signal circled in red shows the NOE-peak corresponding to the olefinic C24-H and the C26 methyl group of (*Z)*-configured γ-oxo-α,β-unsaturated ester **71**. Other prominent NOE-peaks in the same column correspond to the spatial correlations of the olefinic proton with the C21-CH_3 and the two adjacent diastereotopic protons on C22. Noteworthy, the C24-H doesn't show any NOE-peaks with the ethyl-CH_2 and -CH_3, further confirming the (*Z*)-configuration.

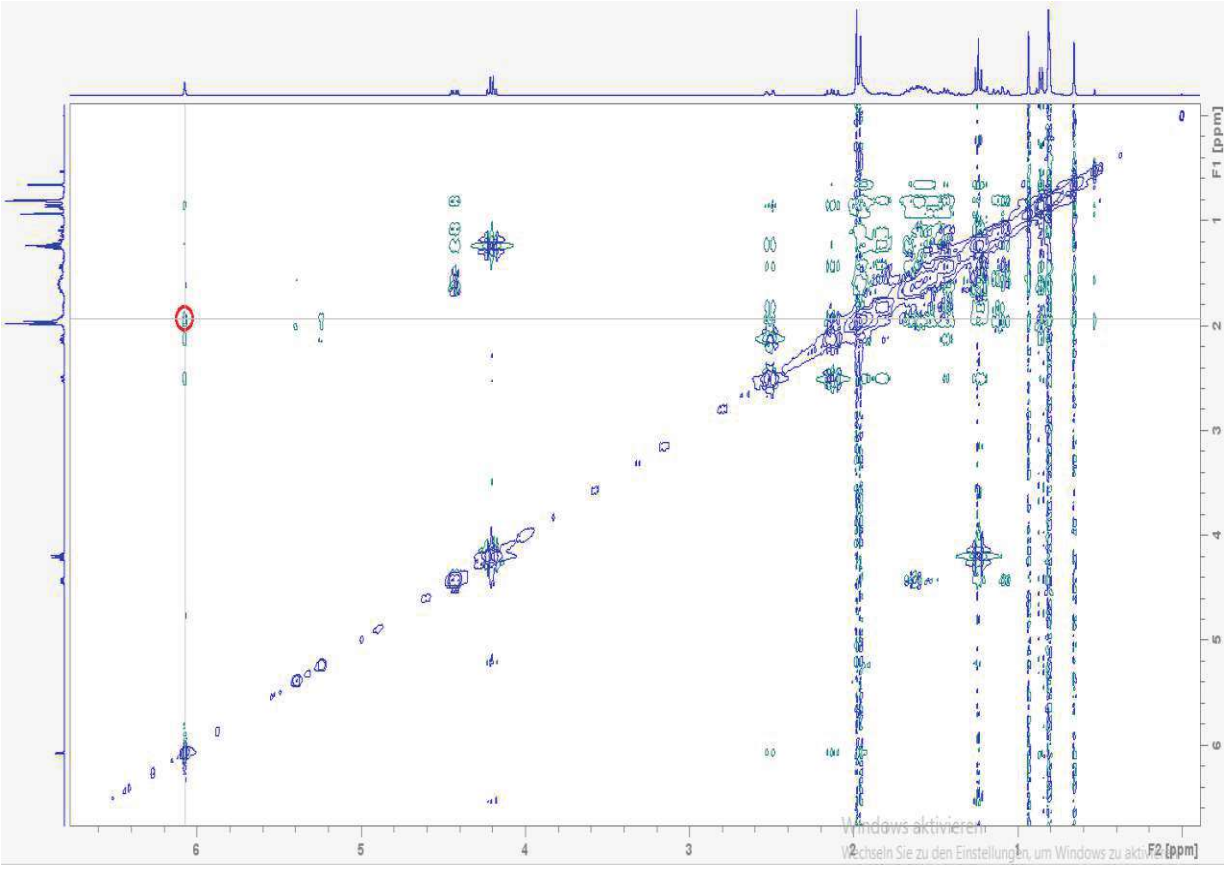

*Figure 9: NOESY spectrum of side product **71***

Signals circled in red show the NOE-Peaks of the C24-H with CH_3 and CH_2 groups, having shifts of 4.25 and 1.33 ppm respectively. Those belong to the ethyl-group γ-oxo-α,β-unsaturated ester **72** further validating the assumed (*E*)-configuration. Other prominent NOE-peaks in the same column show correlations of the olefinic proton with the C21-CH_3 and the two adjacent diastereotopic protons on C22. The C27-methyl group also shows a NOE with the C24-H, but its integral is significantly lower compared to the corresponding correlation in compound **71**.

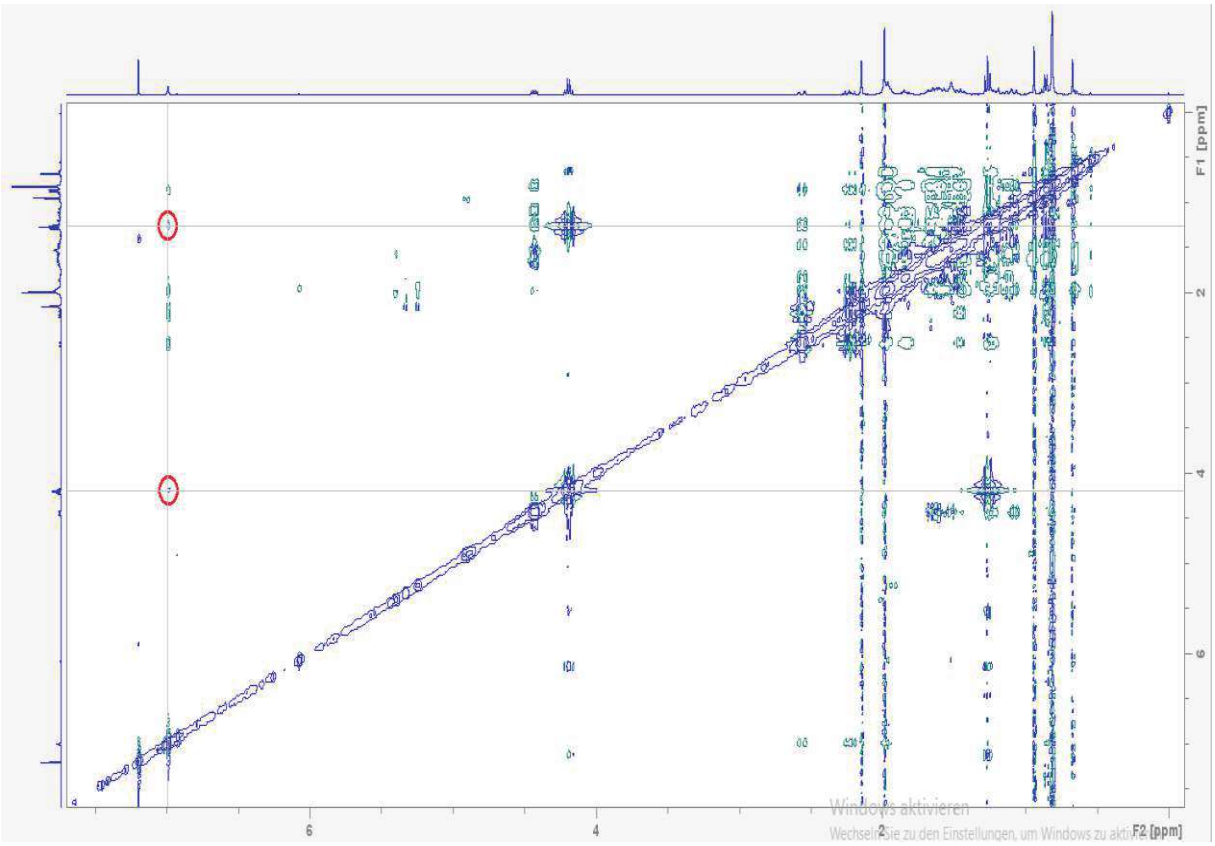

*Figure 10: NOESY spectrum of compound **72***

The problem is that the side product of the Riley oxidation coincides with the (*Z*)-isomer, while the product of the Dess-Martin oxidation coincides with the reported shift of the (*E*)-configured product, but it is not known how the mechanism of the Dess-Martin oxidation could lead to double bond isomerization. The mechanism of the Riley oxidation on the other hand should allow for double bond isomerization, as illustrated below. Both experiments need to be reproduced and also tested with (*E*)-configured starting material and the products characterised more thoroughly for clarification. [5][13][28]

A possible explanation for the formation of different products in the Riley oxidation, containing either an (E)- or (Z)-configured double bond, are illustrated by Scheme 33 below. Pathway A should be generally favoured because of less steric interactions in the transition state, while additional hydrogen bridge bonding could stabilize the transition state in pathway B and explain the formation of the ketone product by activating the C-H bond.

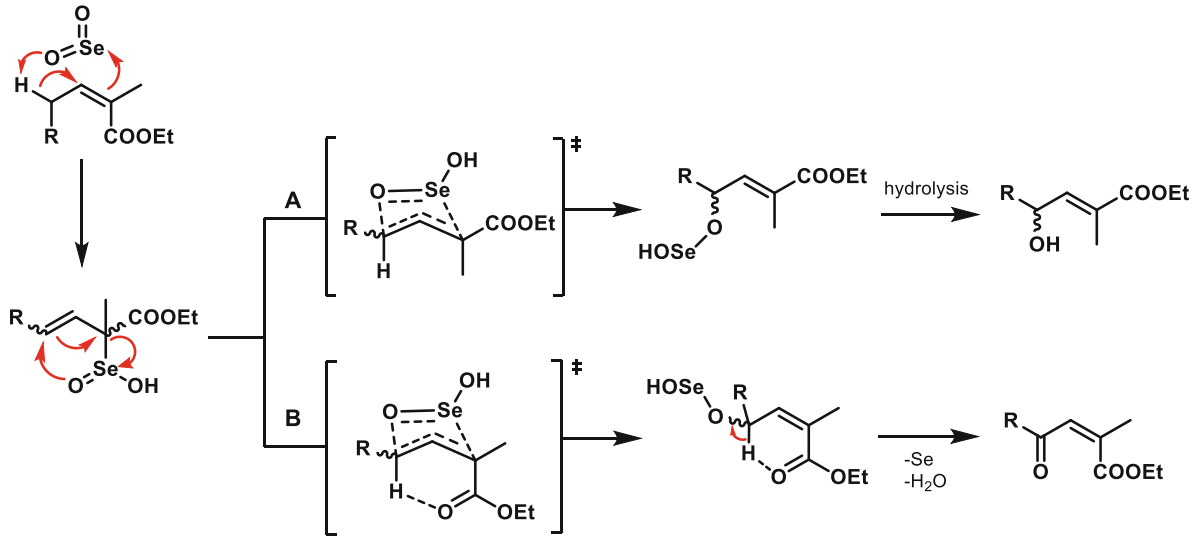

Scheme 33: Possible mechanisms explaining the formation of (E)- and (Z)-configured products

Nonetheless, the hydroxylated products finally allowed for testing of some conditions which could achieve functionalization at C17. Irradiating a solution of γ-hydroxy-α,β-unsaturated ester **70A** with stoichiometric amounts of iodine and lead tetraacetate in carbon tetrachloride with a 250W incandescent light bulb led to formation of a mixture of products, none of which could be identified or isolated in a pure form. [11]

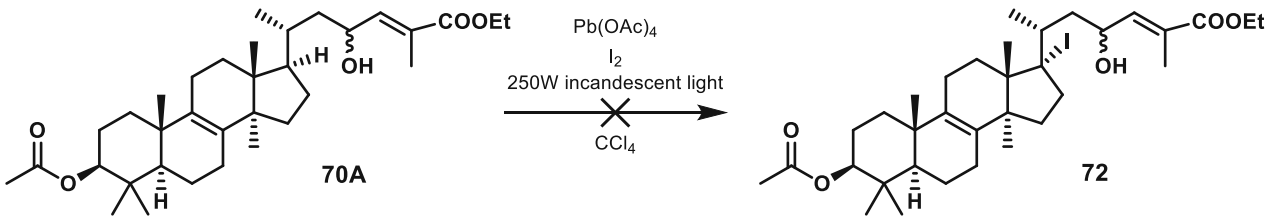

Scheme 34

Stirring the γ-hydroxy-α,β-unsaturated ester **70A** with stoichiometric amounts of iodine and lead tetraacetate in benzene under inert atmosphere, but without additional irradiation, led to formation of one major product which was challenging to identify because of its instability, making it impossible to obtain clean NMR spectra. [11]

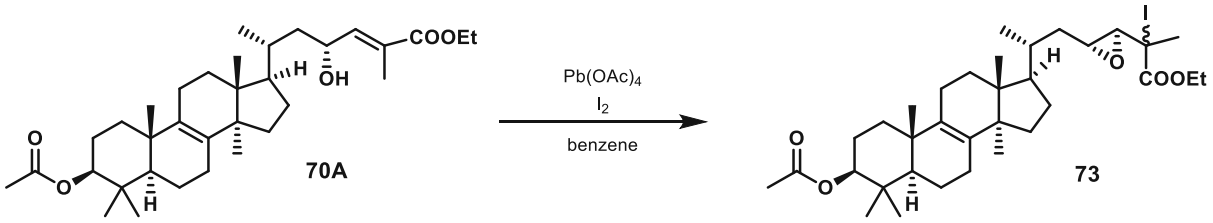

Scheme 35

Solutions of the unstable product turned violet in a short amount of time which indicated the presence of covalently bound iodine. For further investigation, a series of decomposition experiments aiming at the elimination of iodine was conducted. They included heating in DBU, addition of AgOTf and standing at room temperature in a closed flask. Each of those experiments led to the decomposition of the material into several different products. Attempts at purification, such as preparatory TLC, did not allow for a clean NMR spectrum. Only one product could be identified as the one-carbon dehomologated aldehyde by comparison with the aldehyde proton shifts of the corresponding experiment (see section 4.3). In combination with the NMR spectra of the parent compound, this helped to identify the supposed structure **73** depicted above. The arrangement of reactive functionalities in close proximity could easily explain its instability.

As those reactions were only conducted a few times on a small scale with only small variation in conditions and little control over reaction times, there is much room for further improvement. Especially, the experiments need to be repeated with (*Z*)-configured starting material.

5 Outlook and Summary

5.1 Outlook

The γ-hydroxylation of **69** needs to be explored further. The Riley conditions will be tested with (*E*)-configured starting material and, eventually, conditions for double bond isomerization or (*Z*)-selective hydroxylation need to be established.

With the methodology for strategic sidechain oxidations set in place, the way is paved for evaluation of the further key transformations towards Forrestiacid-precursor Neoabiestrine F. With the hydroxyl-group in place, suitable reaction conditions must be found for achieving the desired Csp^3-H functionalization at C17, paving the way for further studies on the rearrangement of the lanostane skeleton.

An alternative way to using a 1,5-HAT for the C17 functionalization is the methodology used by Wu and Deng in their total synthesis of Spirochensilide A (**31**). [13] It has already been discovered by a Bachelor's student in our research group, that the described reaction sequence for the hydroxylation of C17 (see Section 3.1) can be applied to lanosterol derived aldehyde **60**.

Ideally, we aim to be able to functionalize C17 with different leaving groups such as (pseudo-)halides or activated alcohols. From there on a number of different conditions aiming at the desired rearrangement can be examined. There are a number of possibilities for this like Lewis-acid activation, use of Brønsted bases, Ag^+-salts, as well as different solvent systems.

Once this methodology is set in place, all that remains is the deprotection of the C3 hydroxyl group and subsequent oxidation of the alcohols into ketones, forming Neoabiestrine F (**7**) before the final challenge of Diels-Alder reactions can be faced.

Of course, this overview is simplified and there are additional synthetic challenges to explore like the (*E*)/(*Z*)-isomerization or potential isomerization of the double bond in the α,β-unsaturated ester to the exo-position.

5.2 Summary

To conclude, a five-step linear reaction sequence of strategic sidechain oxidations on lanosterol towards Forrestiacids A (**5**) and B (**6**) could be established. All conditions were highly optimized and tested up to a multi-gram scale, with the first four steps giving high to excellent yields. The final transformation, the intricate γ-hydroxylation of α,β-unsaturated ester **69** was facilitated using selenium dioxide, yielding moderate amounts of both diastereomeric alcohols **70A/B** in overall yields of 33% (all isomers), albeit in the undesired (*E*)-configuration.

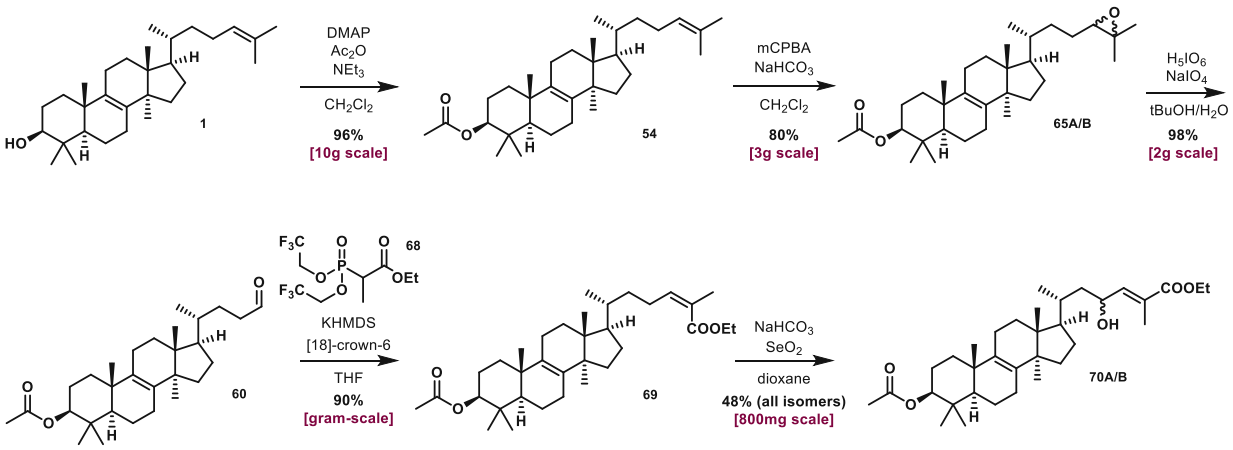

Scheme 36: Established optimized reaction sequence

6 Experimental Part

6.1 General Remarks

Commercial reagents were – unless stated otherwise – used without further purification. Absolute solvents were dried using a PURESOLV facility. Reaction flasks were oven dried at 110°C. For oxygen- and moisture-sensitive reactions, Schlenk technique with a slight overpressure of argon was used. Air- and moisture sensitive liquids and solutions were transferred through rubber septa using syringes. If not specified differently, all reactions were stirred magnetically.

6.1.1 Chromatography

Thin Layer Chromatography

TLC was carried out on silica gel plates on aluminium support (Merck, silica gel 60 F_{254}). The spots were visualized *via* heat staining using a solution of ceric ammonium molybdate in EtOH/H_2SO_4, *p*-anisaldehyde in EtOH/AcOH/H_2SO_4 or $KMnO_4$ and K_2CO_3 in 0.6% aq. NaOH.

Column Chromatography

Preparative column chromatography was performed in glass columns packed with silica gel 60 (Merck, 40-63 µm) under slight overpressure.

6.1.2 Analysis

NMR

NMR measurements were recorded on a Bruker Avance 400 (400 and 100 MHz) or Bruker Avance 600 (600 MHz) instrument. Chemical shifts were reported in parts per million (ppm, δ) relative to using the solvent peak as the internal reference.

Melting Points

Melting Points were measured using a Kofler Hot Stage Microscope or Optimelt MPA100 apparatus.

Optical rotation

The specific rotations were measured on an Anton Parr MCP 500 polarimeter in 1M solution in methylene chloride at 20°C and 589 nm.

6.2 Synthesis of Compounds

6.2.1 (3S,5R,10S,13R,14R,17R)-4,4,10,13,14-pentamethyl-17-((R)-6-methylhept-5-en-2-yl)-2,3,4,5,6,7,10,11,12,13,14,15,16,17-tetradecahydro-1H-cyclopenta[a]phenanthren-3-yl acetate

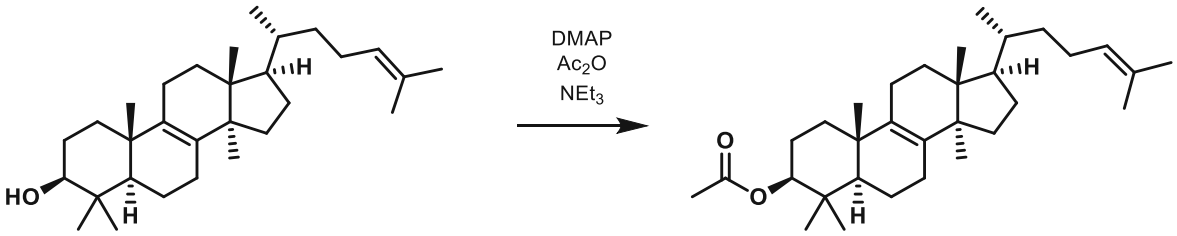

$C_{30}H_{50}O$
426.39
1

$C_{32}H_{52}O_2$
468.40
54

Commercially available lanosterol (**1**) (20 g, 46.87 mmol, 1 eq., approx. 60% pure), triethylamine (17.72 mL, 187.47 mmol, 6 eq.) and DMAP (573 mg, 4.69 mmol, 0.1 eq.) were dissolved in DCM (350 mL) and acetic anhydride (19.14 g, 187.47 mmol, 4 eq.) was added over 5 minutes. After 1 h TLC (PE/EtOAc 2:1) indicated completion and the solution was quenched with sat. aq. $NaHCO_3$-solution (50 mL). The phases were separated, and the aqueous phase was extracted with DCM (3x 120 mL). All the volatiles were evaporated under reduced pressure to yield the crude product (11.444 g). The product was purified *via* flash chromatography (PE:EA 15:1) yielding 20.105 g (92%) of the acetylated product **54** as a white powder.

R_F: 0.77 (PE:EA 10:1)

^{1}H NMR (400 MHz, $CDCl_3$) δ 5.10 (tt, *J* = 7.1, 1.4 Hz, 1H), 4.50 (dd, *J* = 11.5, 4.6 Hz, 1H), 2.07 – 1.80 (m, 10H), 1.77 – 1.56 (m, 11H), 1.54 – 1.24 (m, 7H), 1.18 – 1.09 (m, 3H), 1.00 (s, 3H), 0.92 – 0.85 (m, 13H), 0.69 (s, 3H).

^{13}C NMR (101 MHz, $CDCl_3$) δ 170.97, 134.46, 134.20, 130.87, 125.21, 80.90, 50.47, 50.34, 49.77, 44.44, 37.76, 36.86, 36.31, 36.22, 35.24, 30.93, 30.78, 28.18, 27.87, 26.34, 25.68, 24.88, 24.20, 24.14, 21.29, 20.96, 19.14, 18.59, 18.09, 17.59, 16.49, 15.71. [29]

m.p.: 125°C

α_D^{20}: 48.6° (c 1.0, CH2Cl2)

6.2.2 (3S,5R,10S,13R,14R,17R)-17-((2R)-5,6-dihydroxy-6-methylheptan-2-yl)-4,4,10,13,14-pentamethyl-2,3,4,5,6,7,10,11,12,13,14,15,16,17-tetradecahydro-1H-cyclopenta[a]phenanthren-3-yl acetate

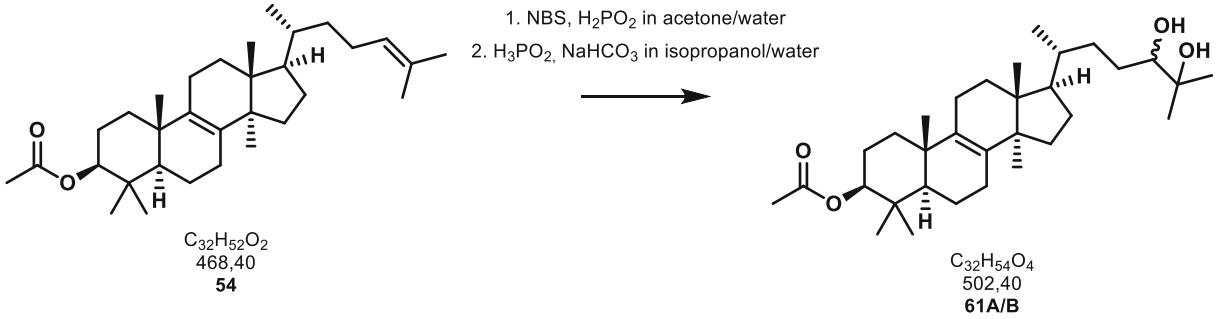

$C_{32}H_{52}O_2$
468,40
54

$C_{32}H_{54}O_4$
502,40
61A/B

The starting material **54** (5g, 10.66 mmol, 1 eq., approx. 60% pure) was dissolved in acetone (450 mL), water (7,5 mL) and hypophosphorous acid (1,35 mL, 50% in water, 12.48 mmol, 2.34 eq.) and *N*-bromosuccinimide (1520 mg, 8.53 mmol, 1.6 eq.) were added. After 10 min of stirring at r.t. $NaHCO_3$ (1480 mg, 17,6 mmol, 3.3 eq.) was added and the mixture was concentrated under vacuum. The residue was then dissolved in isopropanol (150 mL) and water (50 mL) and hypophosphorous acid (3.6 mL, 50% in water, 33.27 mmol, 6.24 eq.), $NaHCO_3$ (2240 mg, 26.67 mmol, 5 eq.) was added and the mixture refluxed for 4 h. The product was precipitated by dilution with water (fast addition on hot solution), filtered of and washed until neutral, then dried and purified *via* flash column chromatography (First, the dihydroderivatives were eluted with DCM, then the product was eluted with EA), yielding 800 mg (30%) of diastereomeric mixture of diols **61A/B** as a white waxy solid.

R_F: 0,41 (PE:EA 2:1)

^{1}H NMR (600 MHz, $CDCl_3$) δ 4.49 (dd, *J* = 11.8, 4.4 Hz, 1H), 3.35 (t, *J* = 6.2 Hz, 0.5H-24*R*), 3.31 – 3.27 (m, 0.5H-24*S*) ,2.04 (s, 7H), 1.96 – 1.89 (m, 1H), 1.73 – 1.63 (m, 6H), 1.58 (ddd, *J* = 12.4, 4.2, 1.8 Hz, 2H), 1.51 – 1.46 (m, 2H), 1.38 (tdd, *J* = 10.7, 8.1, 3.6 Hz, 2H), 1.31 (dd, *J* = 13.7, 3.5 Hz, 1H), 1.20 (s, 3H), 1.18 – 1.10 (m, 6H), 0.99 (d, *J* = 1.3 Hz, 4H), 0.91 – 0.88 (m, 3H), 0.87 – 0.84 (m, 10H), 0.68 (d, *J* = 3.4 Hz, 3H).

^{13}C NMR (151 MHz, $CDCl_3$) δ 171.20, 134.57, 134.37, 81.06, 79.78, 78.90, 73.39, 73.33, 50.69, 50.54, 50.61, 44.63, 44.61, 37.94, 36.89, 36.45, 35.39, 33.67, 33.24, 31.10, 30.93, 28.82, 28.54, 28.45, 28.32, 28.05, 26.74, 26.71, 26.50, 24.40, 24.30, 23.36, 23.28, 21.51, 21.12, 19.33, 18.97, 18.68, 18.25, 16.68, 15.92.

Distinguishable peaks for both isomers (assignment referring to[21]):

(*R*): 78.90 (C24),36.45 (C20), 33.24 (C22), 28.54 (C23) , 18.68 (C21),

(*S*): 79.78 (C24), 36.89 (C20), 33.67 (C22), 28.82 (C23), 18.97 (C21),

Unassigned pairs: 73.39 and 73.33, 50.69 and 50.54, 44.63 and 44.61, 28.36 and 28.28.

m.p.: 185°C

6.2.3 (3S,5R,10S,13R,14R,17R)-4,4,10,13,14-pentamethyl-17-((R)-5-oxopentan-2-yl)-2,3,4,5,6,7,10,11,12,13,14,15,16,17-tetradecahydro-1H-cyclopenta[a]phenanthren-3-yl acetate

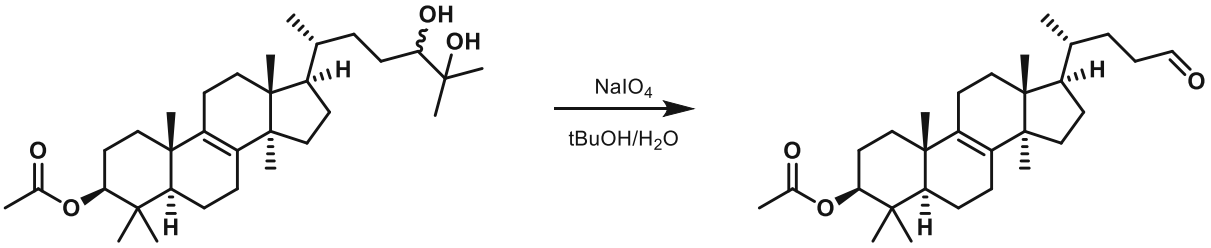

$C_{32}H_{54}O_4$
502,4022
61A/B

$C_{29}H_{46}O_3$
442,3447
60

The diol mixture **61A/B** (750 mg, 1.49 mmol, 1 eq.) was dissolved in tBuOH (35 mL). Sodium *meta*-periodate (479 mg, 2.24 mmol, 1.5 eq.) and water (21 mL) were added and the solution stirred at room temperature. After TLC indicated completion, the tBuOH was evaporated under reduced pressure and the remaining aqueous solution extracted with DCM. The solvent was dried over Na_2SO_4 and evaporated to yield 570 mg (86 %) of the aldehyde **60** as a white solid.

R_F: 0.37 (PE:EA 5:1)

^{1}H NMR (400 MHz, $CDCl_3$) δ 9.77 (t, *J* = 1.9 Hz, 1H), 4.50 (dd, *J* = 11.6, 4.5 Hz, 1H), 2.47 (dddd, *J* = 16.9, 9.7, 5.4, 1.7 Hz, 1H), 2.36 (dddd, *J* = 16.9, 8.8, 6.4, 2.2 Hz, 1H), 2.05 (s, 7H), 1.96 – 1.77 (m, 2H), 1.77 – 1.58 (m, 7H), 1.53 – 1.38 (m, 3H), 1.37 – 1.26 (m, 3H), 1.24 – 1.18 (m, 1H), 1.15 (dd, *J* = 12.6, 2.3 Hz, 1H), 1.00 (s, 3H), 0.92 – 0.82 (m, 12H), 0.71 – 0.67 (m, 3H).

^{13}C NMR (400 MHz, $CDCl_3$): δ 203.39, 171.17, 134.52, 134.46, 81.06, 50.64, 50.44, 49.97, 44.69, 41.29, 37.96, 37.05, 36.18, 35.41, 31.10, 30.92, 28.38, 28.29, 28.06, 26.52, 24.38, 24.32, 21.48, 21.12, 19.34, 18.55, 18.26, 16.68, 15.93.

m.p.: 166°C

α_D^{20}: 57.4° (c 1.0, CH_2Cl_2)

6.2.4 (3S,5R,10S,13R,14R,17R)-17-((2R)-4-(3,3-dimethyloxiran-2-yl)butan-2-yl)-4,4,10,13,14-pentamethyl-2,3,4,5,6,7,10,11,12,13,14,15,16,17-tetradecahydro-1H-cyclopenta[a]phenanthren-3-yl acetate

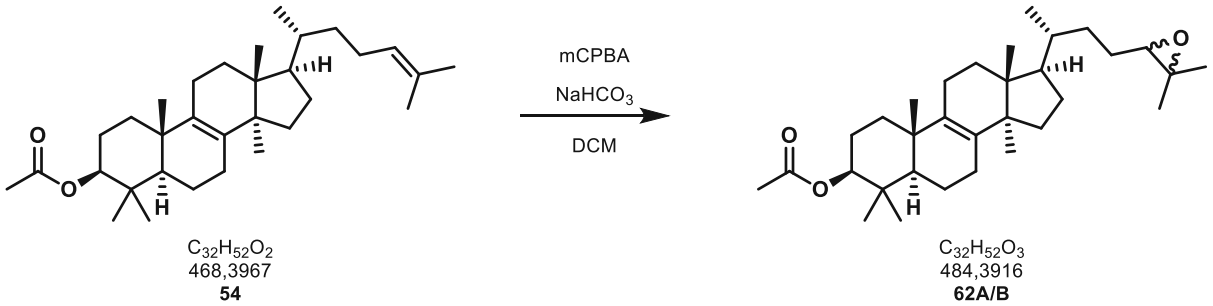

$C_{32}H_{52}O_2$
468,3967
54

$C_{32}H_{52}O_3$
484,3916
62A/B

To a stirred solution of olefinic compound **54** (3g, 6.40 mmol, 1 eq., approx. 60% pure) in DCM (60 mL) at r.t. was added in portions a mixture of $NaHCO_3$ (538 mg, 6.40 mmol, 1 eq.) and mCPBA (828 mg, 4.80 mmol, 0.75 eq.) as follows: half over a period of 30 min at r.t. and half at 0°C over a period of 30 min. The solution was then stirred for another hour at 0°C. Then reaction mixture was then transferred to a separatory funnel and washed three times with 10% aq. $NaHCO_3$-solution. The combined organic phases were dried over Na_2SO_4 and the solvent evaporated to yield the crude which was purified *via* column chromatography (PE:EA 5:1) yielding 1.44 g (80%, assuming starting material is of 60% purity) of the diastereomeric epoxides **62A/B**.

R_F: 0.42 (PE:EA 10:1)

^{1}H NMR (600 MHz, $CDCl_3$) δ 4.50 (dd, *J* = 11.8, 4.4 Hz, 1H), 2.71 – 2.67 (m, 1H), 2.07 – 1.90 (m, 9H), 1.76 – 1.59 (m, 8H), 1.53 – 1.44 (m, 4H), 1.31 (d, *J* = 1.2 Hz, 3H), 1.29 – 1.24 (m, 5H), 1.22 – 1.18 (m, 1H), 1.15 (dt, *J* = 12.6, 1.9 Hz, 1H), 1.00 (s, 3H), 0.91 (d, *J* = 6.3 Hz, 3H), 0.88 (dd, *J* = 5.0, 1.3 Hz, 10H), 0.69 (d, *J* = 0.8 Hz, 3H).

^{13}C NMR (151 MHz, $CDCl_3$) δ 171.18, 134.58, 134.43, 81.08, 65.09, 64.95, 58.57, 58.28, 50.65, 50.53, 50.43, 49.96, 44.64, 37.96, 37.05, 36.50, 36.37, 35.41, 32.96, 32.75, 31.12, 31.09, 30.94, 28.39, 28.34, 28.06, 26.53, 26.08, 25.78, 25.11, 25.09, 24.39, 24.32, 21.49, 21.14, 19.34, 18.90, 18.82, 18.80, 18.72, 18.27, 16.68, 15.91.

Distinguishable signals for the two isomers (assignment referring to [29]):

(R): 64.95 (C24), 58.57 (C25), 50.43 (C17), 36.37 (C20), 32.75 (C22), 31.09 (C12), 28.39 (C16), 25.78 (C23), 25.09 (C26), 18.90 (C27), 18.82 (C21)

(S): 64.09 (C24), 58.28 (C25), 50.53 (C17), 36.50 (C20), 32.96(C22), 31.12 (C12), 28.34 (C16), 25.78 (C23), 25.11 (C26), 18.80 (C27), 18.72 (C21)

m.p.: 163°C

6.2.5 (3S,5R,10S,13R,14R,17R)-4,4,10,13,14-pentamethyl-17-((R)-5-oxopentan-2-yl)-2,3,4,5,6,7,10,11,12,13,14,15,16,17-tetradecahydro-1H-cyclopenta[a]phenanthren-3-yl acetate

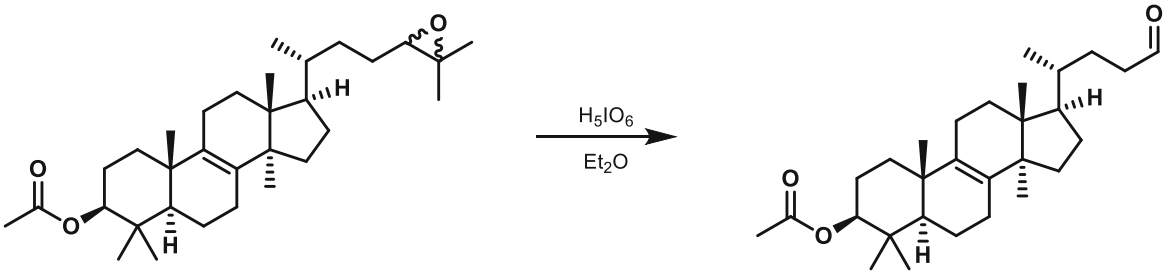

$C_{32}H_{52}O_3$
484,3916
62A/B

$C_{29}H_{46}O_3$
442,3447
60

Epoxides **62A/B** (2g, 4.13 mmol, 1 eq.) were dissolved in a mixture of tBuOH (300 mL) and water (60mL). Periodic acid (940 mg, 4.13 mmol, 1 eq.) and sodium periodate (529 mg, 2.48 mmol, 0.6 eq.) were added and the solution stirred at 40°C. After 2 h the solvent was evaporated under reduced pressure and the residue partitioned by addition of sat. aq. $NaHCO_3$-solution and DCM. The DCM was washed once with water and dried over Na_2SO_4 before solvent evaporation under reduced pressure yielding 1.800 g of aldehyde **60** (98%).

R_F: 0.37 (PE:EA 5:1)

^{1}H NMR (400 MHz, $CDCl_3$) δ 9.77 (t, *J* = 1.9 Hz, 1H), 4.50 (dd, *J* = 11.6, 4.5 Hz, 1H), 2.47 (dddd, *J* = 16.9, 9.7, 5.4, 1.7 Hz, 1H), 2.36 (dddd, *J* = 16.9, 8.8, 6.4, 2.2 Hz, 1H), 2.05 (s, 7H), 1.96 – 1.77 (m, 2H), 1.77 – 1.58 (m, 7H), 1.53 – 1.38 (m, 3H), 1.37 – 1.26 (m, 3H), 1.24 – 1.18 (m, 1H), 1.15 (dd, *J* = 12.6, 2.3 Hz, 1H), 1.00 (s, 3H), 0.92 – 0.82 (m, 12H), 0.71 – 0.67 (m, 3H).

^{13}C NMR (MHz, $CDCl_3$): δ 203.39, 171.17, 134.52, 134.46, 81.06, 50.64, 50.44, 49.97, 44.69, 41.29, 37.96, 37.05, 36.18, 35.41, 31.10, 30.92, 28.38, 28.29, 28.06, 26.52, 24.38, 24.32, 21.48, 21.12, 19.34, 18.55, 18.26, 16.68, 15.93.

m.p.: 166°C

α_D^{20}: 57.4° (c 1.0, CH_2Cl_2)

6.2.6 ethyl (R,Z)-6-((3S,5R,10S,13R,14R,17R)-3-acetoxy-4,4,10,13,14-pentamethyl-2,3,4,5,6,7,10,11,12,13,14,15,16,17-tetradecahydro-1H-cyclopenta[a]phenanthren-17-yl)-2-methylhept-2-enoate

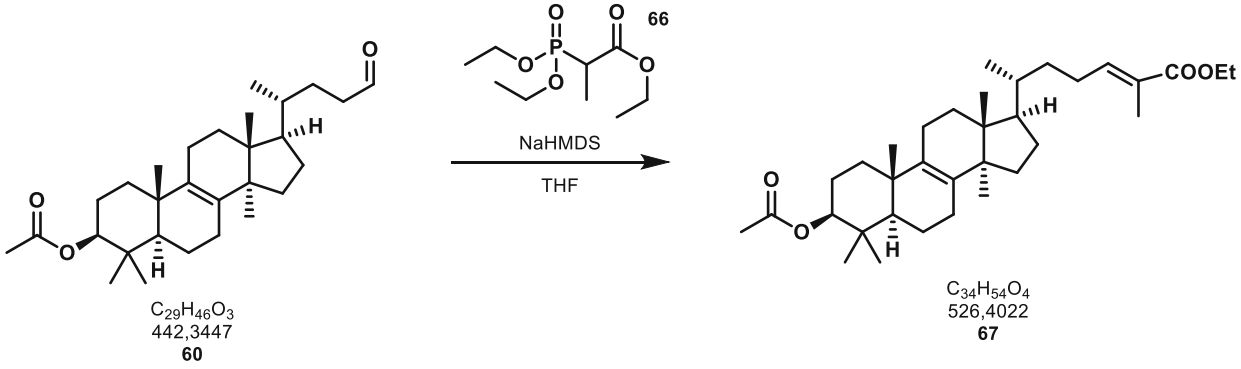

Triethylphosphonopropionate **66** (59 mg, 248.48 µmol, 1.1 eq.) was dissolved in dry THF (3 mL) under argon atmosphere and cooled to -78°C. Then NaHMDS (46 mg, 248.48 µmol, 1.1 eq.) was added dropwise and the reaction stirred for 1h at -78°C. Then the aldehyde **60** (100 mg, 225.89 µmol, 1 eq.) dissolved in THF (1.2 mL) was added dropwise and the mixture stirred for 1h, then allowed to warm to 0°C and quenched with water (1 mL). The mixture was concentrated under reduced pressure, then partitioned by addition of DCM and water and the aqueous phase extracted with DCM. The combined organic extracts were then washed with sat. $NaHCO_3$-solution, sat. aq. NH_4Cl solution and brine. The solvent was evaporated yielding 106 mg (89%) of a mixture of (*E*)- and (*Z*)-isomer, containing 87% of the (*E*)-configured title compound **67** (determined by NMR).

R_F: 0.46 (PE:EA 10:1)

^{1}H NMR (400 MHz, $CDCl_3$) δ 6.75 (td, *J* = 7.4, 1.6 Hz, 1H), 4.50 (dd, *J* = 11.6, 4.5 Hz, 1H), 4.25 – 4.14 (m, 2H), 2.12 – 1.96 (m, 9H), 1.95 – 1.86 (m, 1H), 1.86 – 1.78 (m, 3H), 1.76 – 1.61 (m, 6H), 1.51 (td, *J* = 9.4, 2.2 Hz, 2H), 1.41 (dd, *J* = 9.0, 6.8 Hz, 1H), 1.32 – 1.25 (m, 6H), 1.22 – 1.10 (m, 4H), 1.00 (s, 3H), 0.93 (d, *J* = 6.3 Hz, 3H), 0.89 – 0.86 (m, 9H), 0.69 (d, *J* = 2.0 Hz, 3H).

^{13}C NMR (101 MHz, $CDCl_3$): δ 171.17, 168.43, 143.63, 134.60, 134.43, 126.92, 81.08, 60.17, 50.65, 50.51, 49.96, 44.66, 37.96, 37.05, 36.55, 36.06, 35.42, 31.10, 30.96, 28.36, 28.06, 26.82, 26.53, 24.39, 24.32, 21.48, 21.14, 20.87, 19.33, 18.69, 18.27, 16.68, 15.91, 14.49.

m.p.: 87°C

α_D^{20}: 49.4° (c 1.0, CH_2Cl_2)

6.2.7 ethyl 2-(bis(2,2,2-trifluoroethoxy)phosphoryl)propanoate

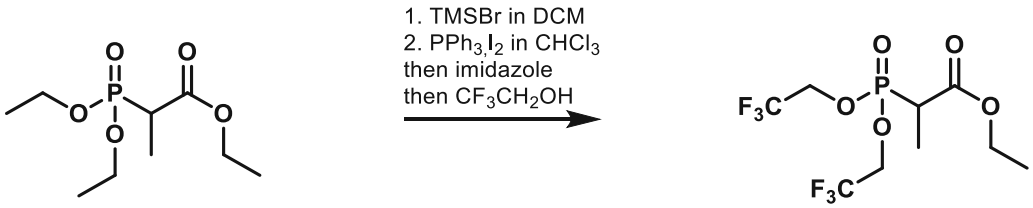

$C_9H_{19}O_5P$
238,0970
66

$C_9H_{13}F_6O_5P$
346,0405
68

To a solution of triethylphosphonopropionate **66** (2g, 8.40 mmol, 1 eq.) in dry DCM (8 mL) under argon atmosphere was added TMSBr (3.21 g, 20.00 mmol, 2.5 eq.) at ice bath temperature. The solution was then stirred for 5 h at r.t. under argon atmosphere. The solution was concentrated *in vacuo* then diluted with methanol (8 mL) and again concentrated. The product was dissolved in $CHCl_3$ (40 mL) and under argon atmosphere at r.t. were added PPh_3 (5.51 g, 20.99 mmol, 2.5 eq.) and I_2 (5.33 g, 20.99 mmol, 2.5 eq.). After 15 min of stirring was added imidazole (5.72 g, 83.59 mmol, 10 eq.), the reaction stirred for 15 min at r.t. and then for 30 min at 50°C. Afterwards trifluoroethanol (3.36 g, 33.58 mmol, 10 eq.) was added and the solution stirred at 60°C for 5h. The solution was filtered and the solvent evaporated to yield the crude product. This was purified *via* column chromatography (PE:EA 5:1 to 2:1) yielding 1.917 g (66%) of the title compound **68** as a clear oil (purification *via* vacuum distillation is also possible).

R_F: 0.45 (PE:EA 5:1)

^{1}H NMR (400 MHz, $CDCl_3$): δ 4.52 – 4.34 (m, 4H), 4.23 (qd, *J* = 7.2, 4.0 Hz, 2H), 3.18 (dq, *J* = 22.7, 7.4 Hz, 1H), 1.52 (dd, *J* = 19.4, 7.4 Hz, 3H), 1.29 (t, *J* = 7.1 Hz, 3H).

^{31}P NMR (162 MHz, $CDCl_3$) δ 23.73.

6.2.8 ethyl (R,Z)-6-((3S,5R,10S,13R,14R,17R)-3-acetoxy-4,4,10,13,14-pentamethyl-2,3,4,5,6,7,10,11,12,13,14,15,16,17-tetradecahydro-1H-cyclopenta[a]phenanthren-17-yl)-2-methylhept-2-enoate

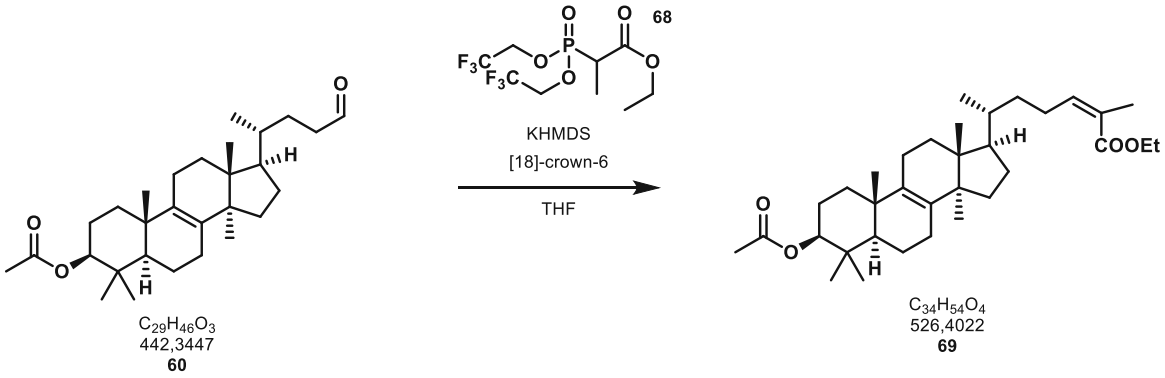

2-[Bis(trifluoroethyl)phosphono]propionic acid ethyl ester (**68**) (1 g, 2.26 mmol, 1 eq.) and [18]-crown-6 (1.79 g, 6.78 mmol, 3 eq.) were dissolved in dry THF (30 mL) under argon atmosphere and cooled to -78°C. Then KHMDS (496 mg, 2.48 mmol, 1.1 eq.) was added dropwise and the reaction stirred for 1h at -78°C. Then the aldehyde **60** dissolved in THF (3 times 5 mL) was added dropwise and the mixture stirred for 30 min at -78°C then allowed to warm to 0°C and quenched by addition of water (60 mL). The mixture was concentrated under reduced pressure, then partitioned by addition of DCM and water (100 mL each) and the aqueous phase extracted with DCM. The combined organic extracts were then washed with sat. $NaHCO_3$-solution, sat. NH_4Cl-solution and water. The crude was purified *via* column chromatography (PE:EA 10:1) yielding 1.066 g (90%) of (*Z*)-isomer **69**.

R_F: 0.51 (PE:EA 10:1)

^{1}H NMR (600 MHz, $CDCl_3$) δ 5.92 – 5.86 (m, 1H), 4.49 (dd, *J* = 11.8, 4.4 Hz, 1H), 4.19 (q, *J* = 7.1 Hz, 2H), 2.54 – 2.44 (m, 1H), 2.40 – 2.31 (m, 1H), 2.04 (s, 7H), 1.94 – 1.89 (m, 1H), 1.88 (t, *J* = 1.4 Hz, 3H), 1.75 – 1.56 (m, 7H), 1.54 – 1.45 (m, 3H), 1.40 (tdd, *J* = 9.5, 6.4, 2.8 Hz, 1H), 1.30 (t, *J* = 7.1 Hz, 5H), 1.19 – 1.08 (m, 3H), 1.00 (s, 3H), 0.91 (d, *J* = 6.4 Hz, 3H), 0.88 – 0.86 (m, 9H), 0.68 (s, 3H).

^{13}C NMR (151 MHz, $CDCl_3$) δ 171.15, 168.40, 143.63, 134.58, 134.41, 126.90, 81.06, 60.15, 50.64, 50.50, 49.95, 44.65, 37.94, 37.03, 36.54, 36.05, 35.40, 31.09, 30.95, 28.35, 28.05, 26.80, 26.52, 24.38, 24.31, 21.47, 21.13, 20.86, 19.32, 18.68, 18.26, 16.67, 15.90, 14.47.

m.p.: 84°C

α_D^{20}: 45.1° (c 1.0, CH_2Cl_2)

6.2.9 ethyl (6R,Z)-6-((3S,5R,10S,13R,14R,17R)-3-acetoxy-4,4,10,13,14-pentamethyl-2,3,4,5,6,7,10,11,12,13,14,15,16,17-tetradecahydro-1H-cyclopenta[a]phenanthren-17-yl)-4-hydroxy-2-methylhept-2-enoate

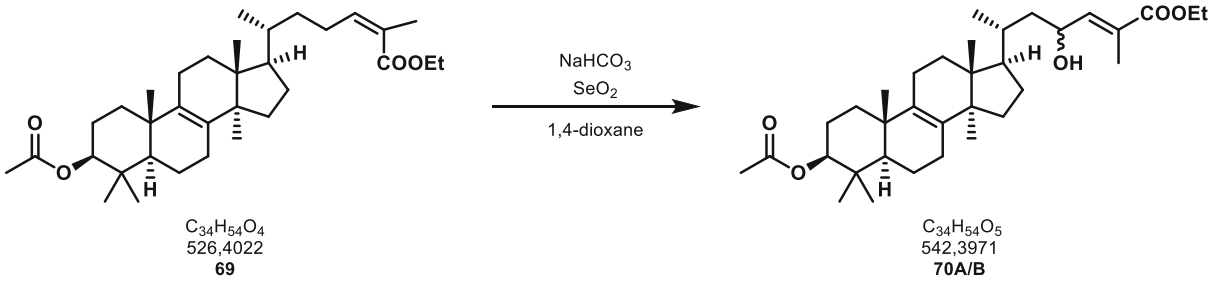

$C_{34}H_{54}O_4$
526,4022
69

$C_{34}H_{54}O_5$
542,3971
70A/B

To a solution of α,β-unsaturated ester **69** (800 mg, 1.52 mmol, 1 eq.) in dioxane (80 mL) were added $NaHCO_3$ (510 mg, 6.07 mmol, 4 eq.) and SeO_2 (506 mg, 4.56 mmol, 3 eq.) subsequently. The mixture was stirred at 100°C for 2h. The reaction was quenched by addition of sat. aq. $Na_2S_2O_3$-solution, extracted with ethyl acetate and the organic phases washed with brine, then dried over Na_2SO_4 and the solvent evaporated. The crude product was purified *via* column chromatography (PE:EA 6:1) to yield two separate diastereomers **70A** 222 mg (27%) and **70B** 222 mg (27%).

A)

R_F: 0.44 (PE:EA 10:1)

^{1}H NMR (400 MHz, $CDCl_3$) δ 6.69 (dq, *J* = 8.2, 1.5 Hz, 1H), 4.58 (ddd, *J* = 10.5, 8.2, 2.7 Hz, 1H), 4.49 (dd, *J* = 11.5, 4.6 Hz, 1H), 4.19 (qd, *J* = 7.2, 1.1 Hz, 2H), 2.09 – 1.90 (m, 8H), 1.86 (d, *J* = 1.5 Hz, 3H), 1.78 – 1.62 (m, 8H), 1.57 – 1.43 (m, 3H), 1.39 – 1.32 (m, 1H), 1.29 (t, *J* = 7.1 Hz, 4H), 1.22 – 1.12 (m, 2H), 1.08 – 1.03 (m, 1H), 1.00 (d, *J* = 4.5 Hz, 6H), 0.87 (dd, *J* = 6.8, 1.1 Hz, 9H), 0.72 (s, 3H).

^{13}C NMR (101 MHz, $CDCl_3$): δ 171.18, 168.11, 144.05, 134.51, 134.45, 127.53, 81.07, 66.37, 60.88, 50.98, 50.63, 50.04, 44.79, 43.23, 37.94, 37.04, 35.40, 32.96, 31.15, 30.91, 28.56, 28.05, 26.50, 24.31 (2C), 21.47, 21.12, 19.33, 18.63, 18.24, 16.67, 15.97, 14.38, 12.82.

m.p.: 178°C

α_D^{20}: 52.1° (c 1.0, CH_2Cl_2)

B)

R_F: 0.34 (PE:EA 10:1)

^{1}H NMR (400 MHz, $CDCl_3$) δ 6.59 (dq, *J* = 9.1, 1.4 Hz, 1H), 4.57 (td, *J* = 8.8, 5.2 Hz, 1H), 4.49 (dd, *J* = 11.6, 4.5 Hz, 1H), 4.21 (qd, *J* = 7.1, 0.8 Hz, 2H), 2.09 – 1.92 (m, 8H), 1.89 (d, *J* = 1.4 Hz, 3H), 1.75 – 1.59 (m, 8H), 1.54 – 1.48 (m, 2H), 1.45 – 1.40 (m, 1H), 1.30 (t, *J* = 7.1 Hz, 6H), 1.19 – 1.11 (m, 2H), 1.01 – 0.95 (m, 6H), 0.87 (d, *J* = 3.3 Hz, 9H), 0.66 (s, 3H).

^{13}C NMR (101 MHz, $CDCl_3$) δ 171.17, 168.13, 142.98, 134.48, 134.45, 129.21, 81.06, 67.50, 60.93, 51.13, 50.62, 49.98, 44.67, 44.02, 37.94, 37.03, 35.39, 34.10, 31.09, 30.91, 28.64, 28.05, 26.49, 24.34, 24.30, 21.47, 21.10, 19.93, 19.32, 18.24, 16.66, 15.84, 14.37, 13.17.

m.p.: 159°C

$\boldsymbol{\alpha_D^{20}}$**:** 61.2° (c 1.0, CH_2Cl_2)

6.2.10 (3S,5R,10S,13R,14R,17R)-17-((R,E)-7-hydroxy-6-methylhept-5-en-2-yl)-4,4,10,13,14-pentamethyl-2,3,4,5,6,7,10,11,12,13,14,15,16,17-tetradecahydro-1H-cyclopenta[a]phenanthren-3-yl acetate

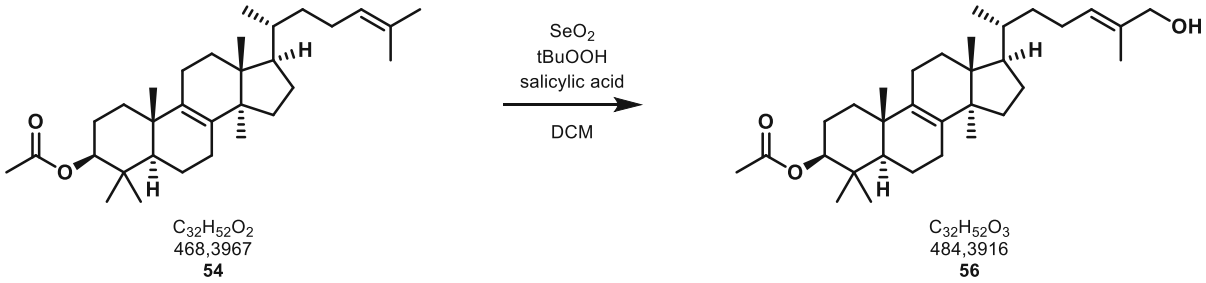

$C_{32}H_{52}O_2$
468,3967
54

$C_{32}H_{52}O_3$
484,3916
56

SeO_2 (2.4 mg, 21.33 µmol, 0.1 eq.) and salicylic acid (3 mg, 21.33 µmol, 0.1 eq.) were dissolved in DCM (12 mL) and cooled to 0°C before adding tBuOOH (5.5M in decane, 155 µL, 853.30 µmol, 4 eq.). Then the starting material **54** was added (100 mg, 213.33 µmol, 1 eq., approx. 60% pure) and the mixture stirred at r.t. for 24 hours. After 24 h the reaction was quenched with sat. aq. Na_2CO_3-solution, extracted with DCM, the organic phases dried over Na_2SO_4 and the solvent evaporated to give the crude product as a white waxy solid which was further purified by column chromatography (PE:EA 10:1) yielding 20 mg (19%) of title compound **56**.

R_F: 0.37 (PE:EA 5:1)

^{1}H NMR (600 MHz, $CDCl_3$) δ 5.39 (tq, *J* = 7.2, 1.4 Hz, 1H), 4.50 (dd, *J* = 11.8, 4.4 Hz, 1H), 4.00 (s, 2H), 2.12 – 2.07 (m, 1H), 2.05 (s, 7H), 1.95 – 1.88 (m, 2H), 1.74 – 1.65 (m, 8H), 1.61 – 1.56 (m, 2H), 1.48 (dddd, *J* = 18.1, 9.6, 7.5, 2.6 Hz, 3H), 1.41 – 1.37 (m, 1H), 1.34 – 1.29 (m, 2H), 1.18 – 1.12 (m, 2H), 1.07 (dddd, *J* = 13.5, 10.4, 8.8, 5.1 Hz, 1H), 1.00 (s, 3H), 0.92 (d, *J* = 6.4 Hz, 3H), 0.87 (dd, *J* = 5.7, 1.1 Hz, 9H), 0.68 (s, 3H).

^{13}C NMR (151 MHz, $CDCl_3$) δ 171.20, 134.57, 134.43, 134.38, 127.23, 81.06, 69.28, 50.61, 50.48, 49.94, 44.62, 37.94, 37.02, 36.43, 36.10, 35.39, 31.08, 30.94, 28.36, 28.05, 26.51, 24.65, 24.39, 24.31, 21.51, 21.13, 19.33, 18.74, 18.25, 16.68, 15.90, 13.80.

m.p.: 126°C

α_D^{20}: 55.7° (c 1.0, CH_2Cl_2)

6.2.11 (3S,5R,10S,13R,14R,17R)-4,4,10,13,14-pentamethyl-17-((R,E)-6-methyl-7-oxohept-5-en-2-yl)-2,3,4,5,6,7,10,11,12,13,14,15,16,17-tetradecahydro-1H-cyclopenta[a]phenanthren-3-yl acetate

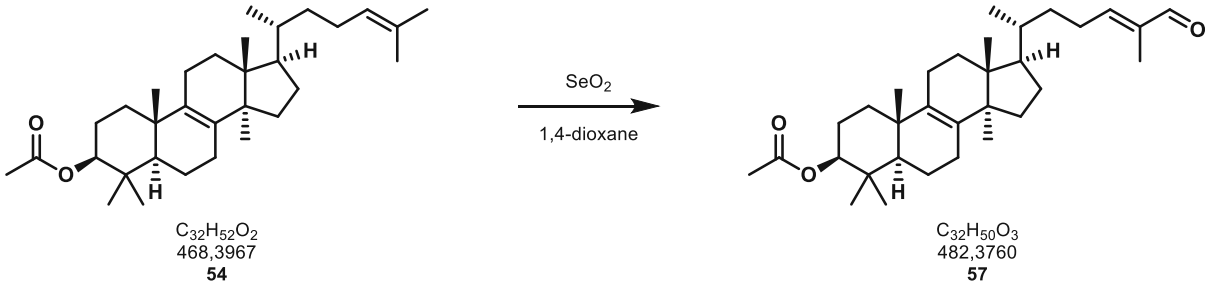

$C_{32}H_{52}O_2$
468,3967
54

$C_{32}H_{50}O_3$
482,3760
57

Selenium dioxide (26 mg, 234.66 µmol, 1.1 eq.) was dissolved in dry 1,4-dioxane (12 mL), followed by addition of the starting material **54** (100 mg, 213.33 µmol, 1 eq., approx. 60% pure). The mixture was stirred at 60°C overnight under the exclusion of air moisture. The reaction was then quenched by cautious addition of sat. $NaHCO_3$-solution and extracted with ethyl acetate, the organic phases then washed with brine, dried over Na_2SO_4 and the solvent evaporated to give the crude product which was further purified by column chromatography (PE:EA 10:1) to yield 60 mg (58%) of α,β-unsaturated aldehyde **57** as a white solid.

R_F: 0.38 (PE:EA 10:1)

^{1}H NMR (400 MHz, $CDCl_3$) δ 9.39 (s, 1H), 6.53 – 6.44 (m, 1H), 4.50 (dd, *J* = 11.6, 4.5 Hz, 1H), 2.39 (ddd, *J* = 15.7, 10.0, 5.7 Hz, 1H), 2.31 – 2.18 (m, 1H), 2.03 (s, 7H), 1.98 – 1.87 (m, 1H), 1.75 (d, *J* = 1.2 Hz, 4H), 1.68 (ddd, *J* = 12.2, 6.8, 3.1 Hz, 4H), 1.59 (ddd, *J* = 12.0, 7.4, 3.3 Hz, 3H), 1.54 – 1.39 (m, 3H), 1.36 – 1.28 (m, 2H), 1.22 – 1.11 (m, 3H), 1.00 (s, 3H), 0.95 (d, *J* = 6.2 Hz, 3H), 0.88 (s, 9H), 0.69 (s, 3H).

^{13}C NMR (101 MHz, $CDCl_3$) δ 195.54, 171.15, 155.71, 139.24, 134.50, 134.48, 81.04, 50.64, 50.45, 49.97, 44.71, 37.95, 37.05, 36.51, 35.41, 34.92, 31.11, 30.92, 28.40, 28.05, 26.52, 26.18, 24.38, 24.31, 21.47, 21.12, 19.34, 18.64, 18.25, 16.67, 15.92, 9.30.

m.p.: 164°C

α_D^{20}: 52.8° (c 1.0, CH_2Cl_2)

7 Bibliography

[1] Hill, R. A.; Connolly, J. D. *Nat. Prod. Rep*. **2020**, 37 (7), 962–998.

[2] Zhang, S.-S.; Wang, Y.-G.; Ma, Q.-Y.; Huang, S.-Z.; Hu, L.-L.; Dai, H.-F.; Yu, Z.-F.; Zhao, Y.-X. *Molecules* **2015**, 20 (2), 3281–3289.

[3] Ren, Y.-H.; Liu, Q.-F.; Chen, L.; He, S.-J.; Zuo, J.-P.; Fan, Y.-Y.; Yue, J.-M. *Org. Lett.* **2019**, 21 (6), 1904–1907.

[4] Xiong, J.; Zhou, P.; Jiang, H.; Huang, T.; He, Y.; Zhao, Z.; Zang, Y.; Choo, Y.; Wang, X.; Chittiboyina, A. G.; Pandey, P.; Hamann, M. T.; Li, J.; Hu, J. *Angew Chem Int Ed* **2021**, *60* (41), 22270–22275.

[5] Raldugin, V.A., Shevtsov, S.A., Roshchin, V.I. et al. *Chemistry of Natural Compounds* **1998**, 24, 694–698.

[6] Yong-Li Li, Yan-Xia Gao, Xian-Wen Yang, Hui-Zi Jin, Ji Ye, Luke Simmons, Ning Wang, Andre Steinmetz, Wei-Dong Zhang, *Phytochemistry* **2012**, 81, 159-164.

[7] Peng-Jun Zhou, Ting Huang, Guang-Lei Ma, Ying-Peng Tong, Wen-Xue Chen, Yi Zang, Juan Xiong, Jia Li, and Jin-Feng Hu, *Journal of Natural Products* **2023**, 86 (5), 1251-1260.

[8] Zhou, P.-J.; Zang, Y.; Li, C.; Yuan, L.; Zeng, H.; Li, J.; Hu, J.-F.; Xiong, J. F. *Chinese Chemical Letters* **2022**, 33 (9), 4264–4268.

[9] Karle, I.L. *Acta Cryst*. **1972**. B28, 2000-2007

[10] a) https://www.biozol.de/de/product/USB-453705 (15/09/2024)
b) https://cymitquimica.com/de/produkte/TR-L375910/79-54-9/levopimaric-acid/ (15/09/2024)

[11] Majetich, G.; Wheless, K. *Tetrahedron* **1995**, *51* (26), 7095–7129.

[12] Landaeta Aponte, R. A.; Luxenburger, A.; Cameron, S. A.; Weymouth-Wilson, A.; Furneaux, R. H.; Harris, L. D.; Compton, B. J. *Molecules* **2022**, 27 (7), 2364.

[13] Long, X.; Li, J.; Gao, F.; Wu, H.; Deng, J. *J. Am. Chem. Soc.* **2022**, 144 (36), 16292–16297.

[14] a) Walling, C.; Padwa, A. *J. Am. Chem. Soc.* 1961, 83, 2207. b) Walling, C.; Padwa, A. *J. Am. Chem. Soc.* **1963**, 85, 1597.

[15] Bogan, P.; Gall, R. E. *Aust. J. Chem.* **1979**, 32, 2323.

[16] Condakes, M. L.; Hung, K.; Harwood, S. J.; Maimone, T. J., *J. Am. Chem. Soc.* **2017**, 139 (49), 17783–17786.

[17] Luo, M.; Zhu, S.; Shi, C.; Du, Y.; Yang, C.; Guo, L.; Xia, W. *Org. Lett*. **2022**, 24 (36), 6560–6565.

[18] Xu, S., Norton, R. A., Crumley, F. G. & Nes, W. D. *Journal of Chromatography A* **1998** 452, 377–398.

[19] Marker, R. E.; Wittle, E. L.; Mixon, L. W. *J. Am. Chem. Soc.* 1937, 59 (7), 1368–1373.

[20] Stephenson, L. M.; Speth, D. R. *Org. Chem.* **1979**, 44 (25), 4683–4689.

[21] Kavtaradze, L. K.; Manley-Harris, M.; Nicholson, B. K. *Steroids* **2004**, *69* (10), 697–700.

[22] Sagimori, I.; Yoshioka, H.; Hashimoto, Y.; Ohgane, K. *Bioorganic & Medicinal Chemistry* **2020**, *28* (3), 115298.

[23] Uyanik, M.; Suzuki, D.; Yasui, T.; Ishihara, K. *Angew Chem Int Ed* **2011**, 50 (23), 5331–5334.

[24] Hayashi, Y.; Yamaguchi, J.; Sumiya, T.; Hibino, K.; Shoji, M. J. *Org. Chem.* **2004**, 69 (18), 5966–5973.

[25] Sun, H.; Yang, C.; Gao, F.; Li, Z.; Xia, W. *Org. Lett.* **2013**, 15 (3), 624–627.

[26] Sano, S.; Matsumoto, T.; Toguchi, M., Nakao, M. *SynLett* **2018**, 29(11), 1461-1464

[27] Zheng, C.-Y.; Yue, J.-M. *Nat Commun* **2023**, 14 (1), 2399.

[28] Raldugin, V. A.; Shakirov, M. M.; Leibyuk, T. V. Shevtsov, S. A.; *Chemistry of Natural Compounds* **1991**, 27 (4), 444-449

[29] Emmons GT, Wilson WK, Schroepfer GJ, *Magn Res Chem* **1989**, 27, 1012–24.

8 Appendices

8.1 Abbreviations

Ac	acetyl
AcOH	Acetic acid
AgOTf	Silver triflate
aq.	aqueous
b.r.s.m.	based on recovered starting material
^{t}BuOOH	Tert-butyl hydroperoxide
$CHCl_3$	Chloroform
$(COCl)_2$	Oxalyl chloride
CuI	Copper(I)iodide
DBU	1,8-diazabicyclo[5.4.0]undec-7-ene
DCM	Dichloromethane
DMAP	N,N-Dimethylpyridine-4-amine
DMF	Dimethylformamide
DMP	Dess-Martin-periodinane
EA	Ethyl acetate
EtOH	Ethanol
Et_2O	Diethyl ether
eq.	equivalent(s)
EWG	Electron-withdrawing group
g	gram(s)
HAT	Hydrogen Atom Transfer
HWE	Horner-Wadsworth-Emmons
I_2	Iodine
H_2SO_4	Sulphuric acid
K_2CO_3	Potassium carbonate
KHMDS	Potassium bis(trimethylsilyl)amide
$KMnO_4$	Potassium permanganate
L	liter
$LiAl(OtBu)_3H$	Lithium tri-tert-butoxyaluminum hydride
LTA	Lead tetraacetate
mCPBA	meta-chloroperoxybenzoic acid
NaHMDS	Sodium bis(trimethylsilyl)amide
Na_2CO_3	Sodium carbonate
NaOH	Sodium hydroxide
Na_2SO_4	Sodium sulphate
$Na_2S_2O_3$	Sodium thiosulfate
NMO	N-methylmorpholine N-oxide
NOESY	Nuclear Overhauser and Exchange Spectroscopy
NMR	Nuclear magnetic resonance
Oxone	$2KHSO_5 \cdot KHSO_4 \cdot K_2SO_4$

PE	Petroleum ether
PIDA	Phenyl-λ^3-iodanediyl diacetate
PPh_3	Triphenyl phosphine
pTSA	para-Toluenesulfonic acid
$RuCl_3$	Ruthenium(III)chloride
$Ru(bpy)_3Cl_2$	Ruthenium(II)tris bipyridyl dichloride
sat.	saturated
SeO_2	Selenium dioxide
*t*BuOOH	*tert*-butylhydroperoxide
TBS	tert-butyldimethylsilyl
TBSBr	tert-butyldimethylsilyl bromide
TBSOTf	tert-butyldimethylsilyl triflate
THF	Tetrahydrofuran
TLC	thin layer chromatography
TMS	Trimethylsilane/trimethylsilyl
TMSBr	Trimethylsilyl bromide
TMS	Trimethylsilyl cyanide
[18]-crown-6	1,4,7,10,13,16-hexaoxacyclooctadecane

8.2 Selected Spectra

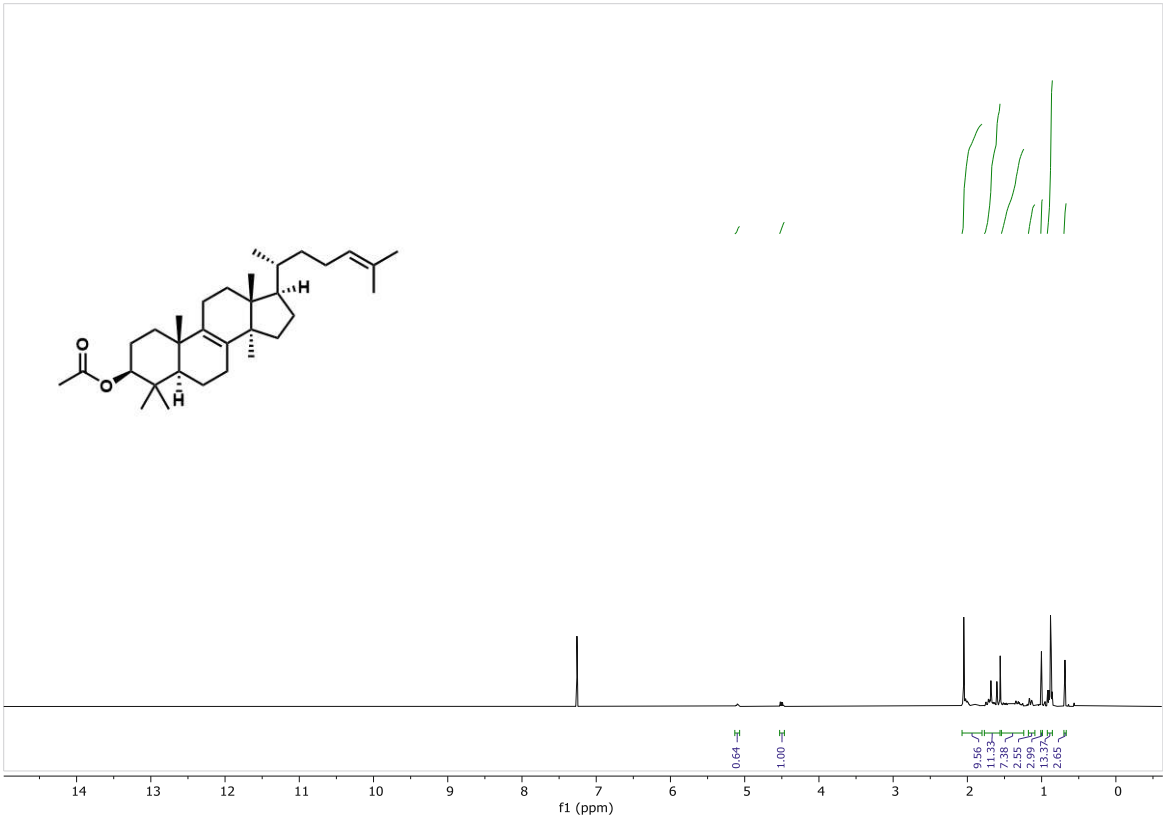

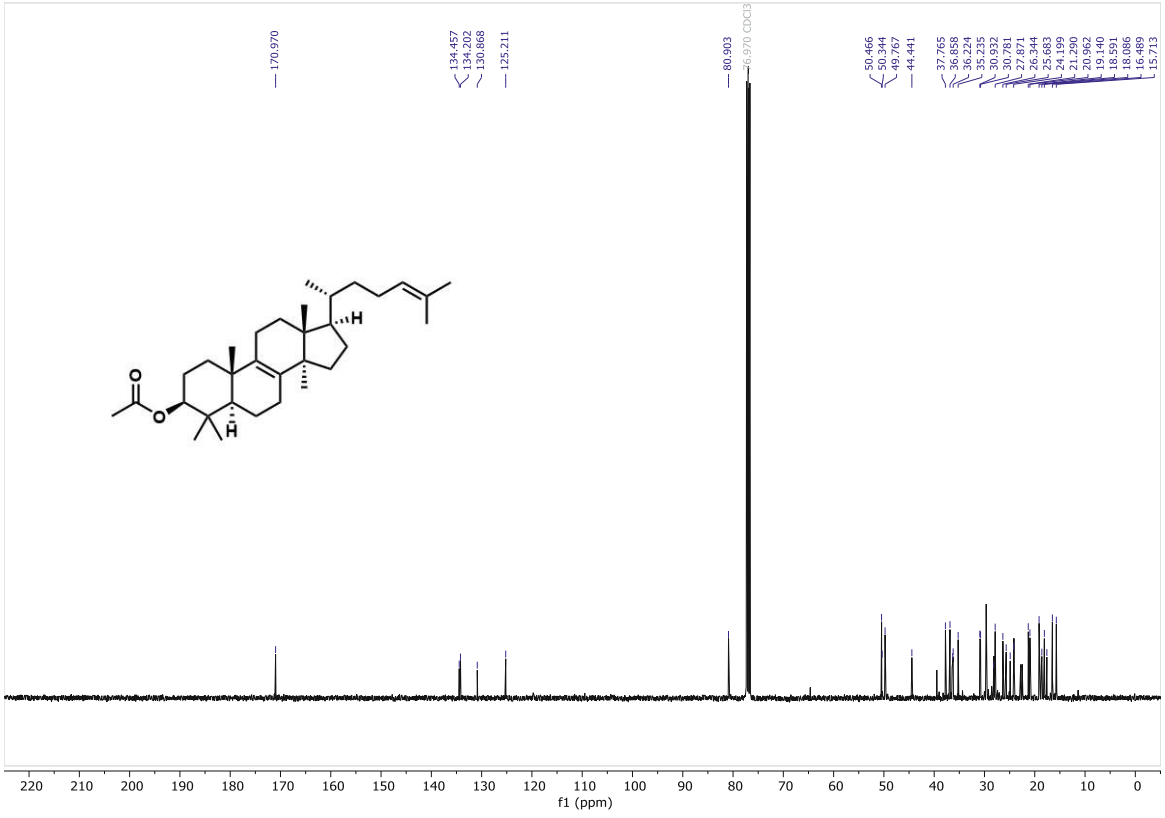

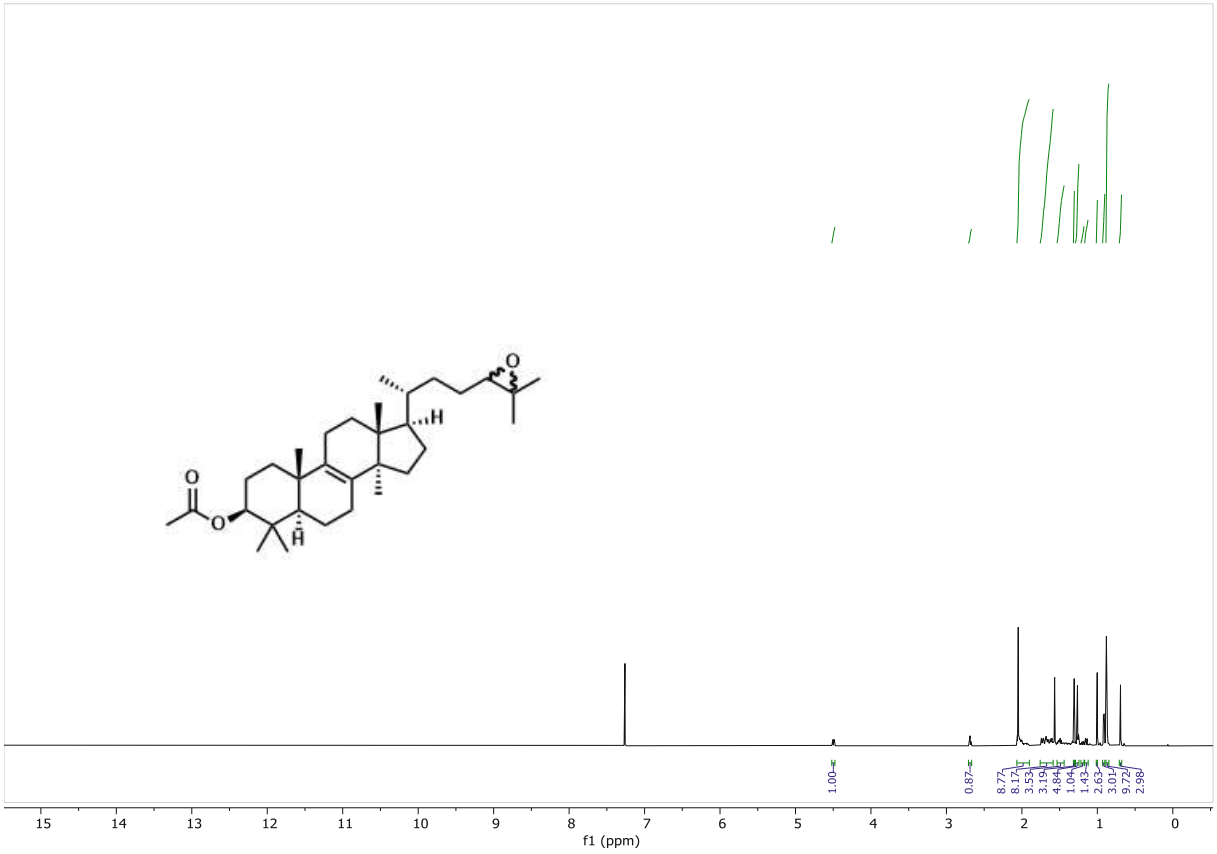

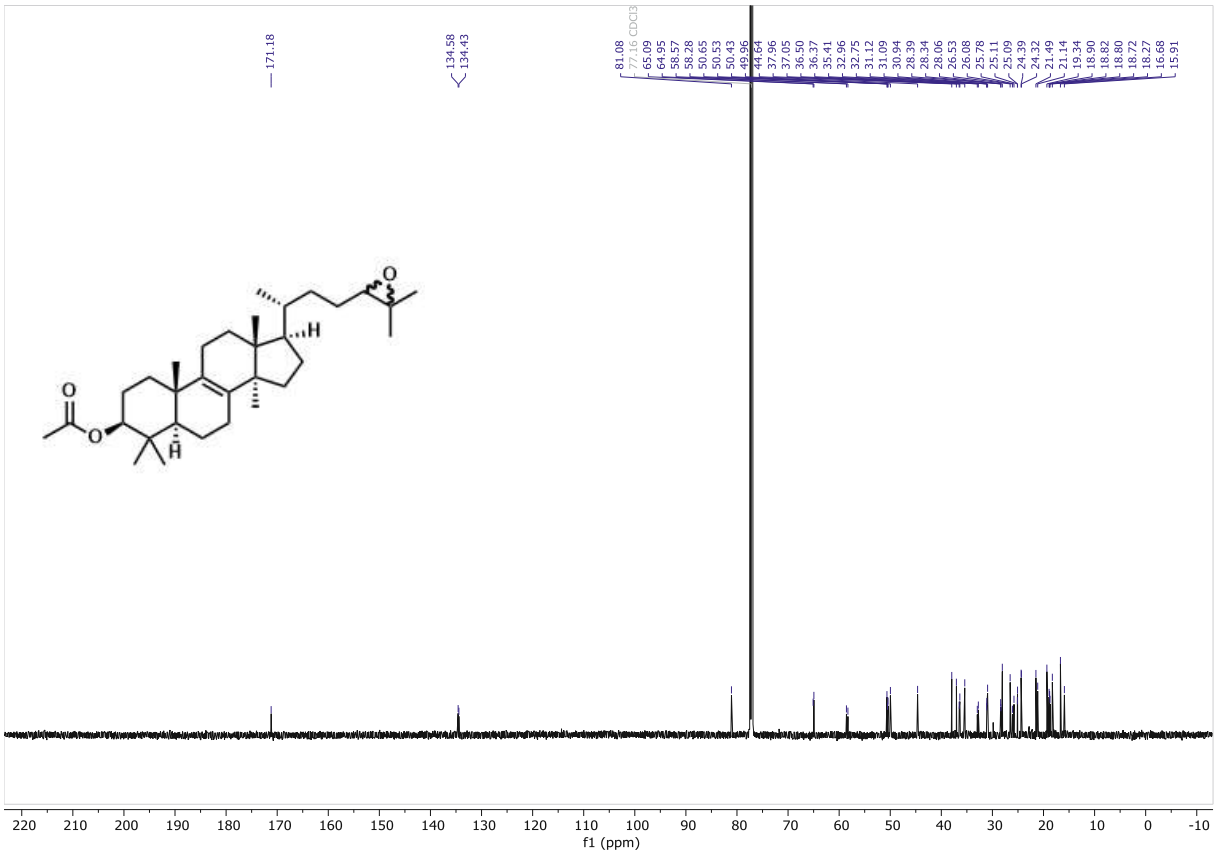

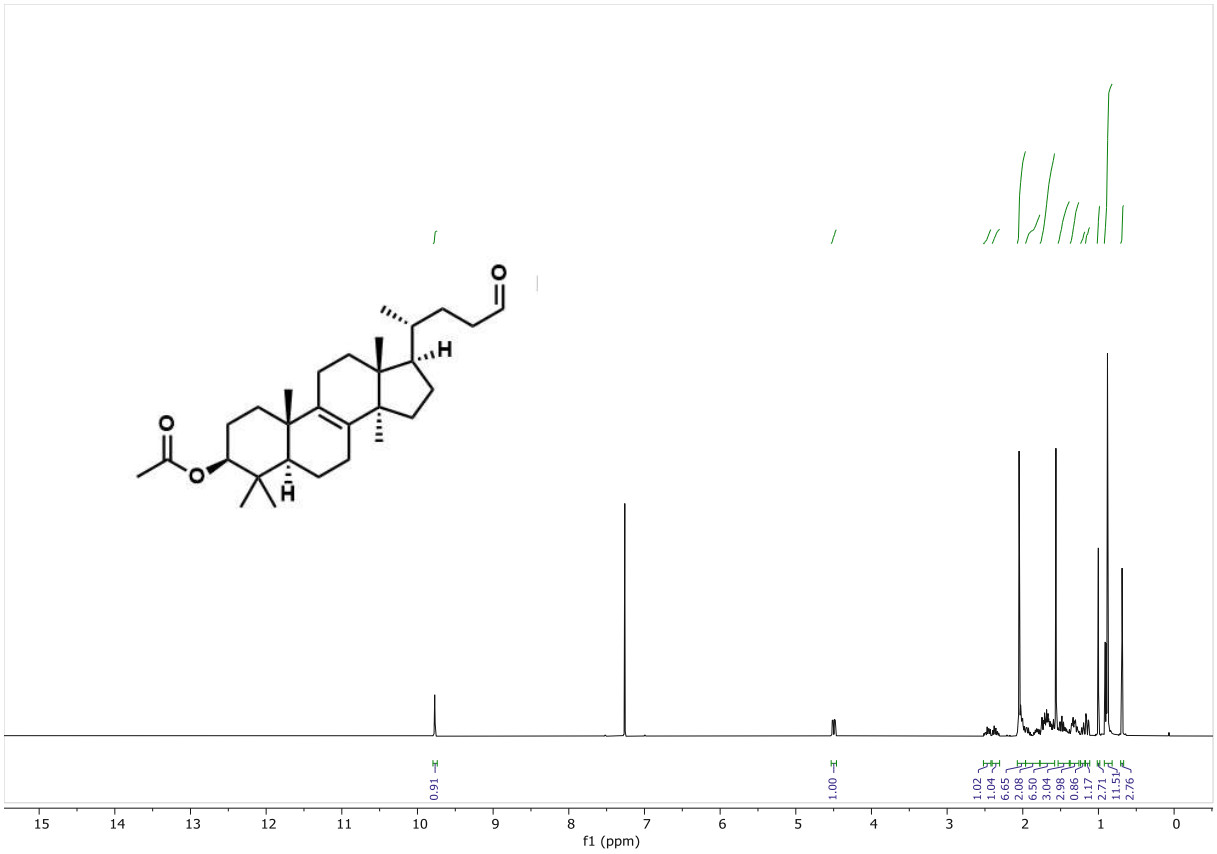

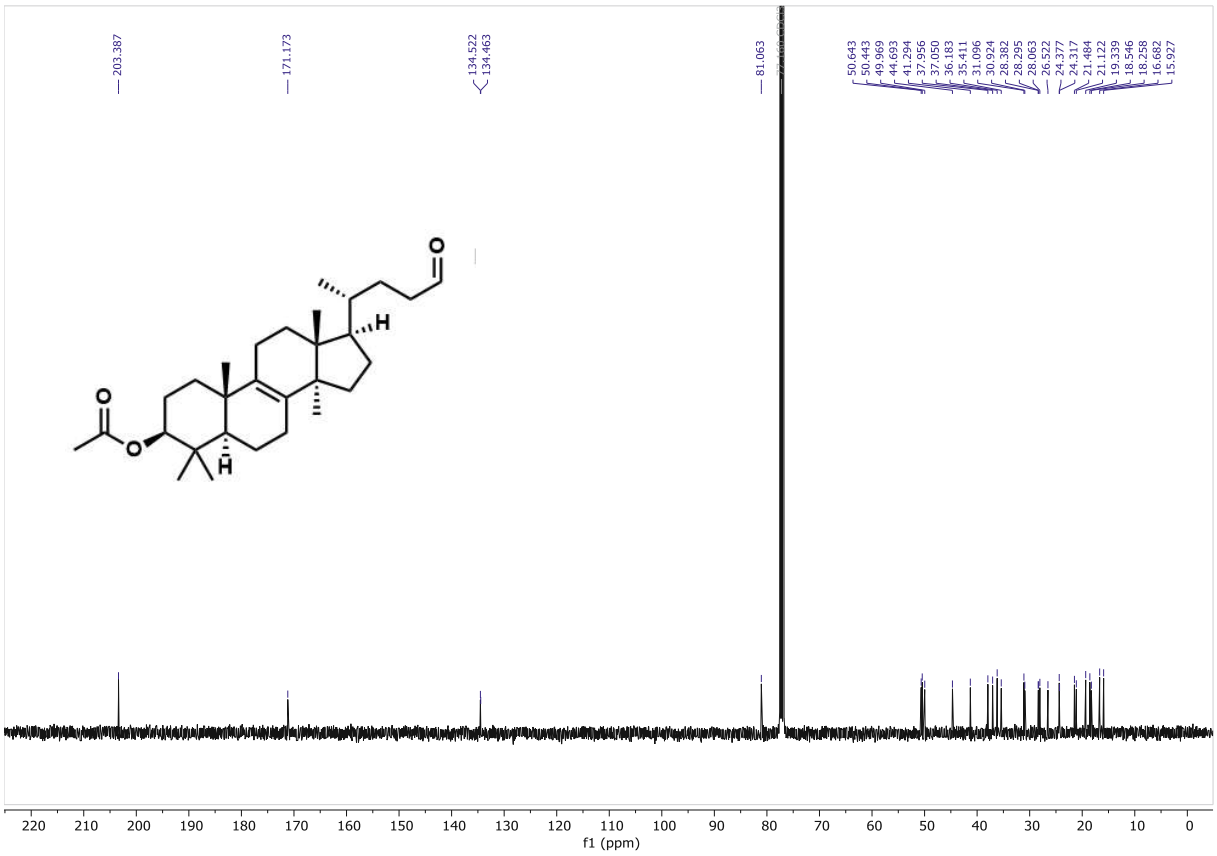

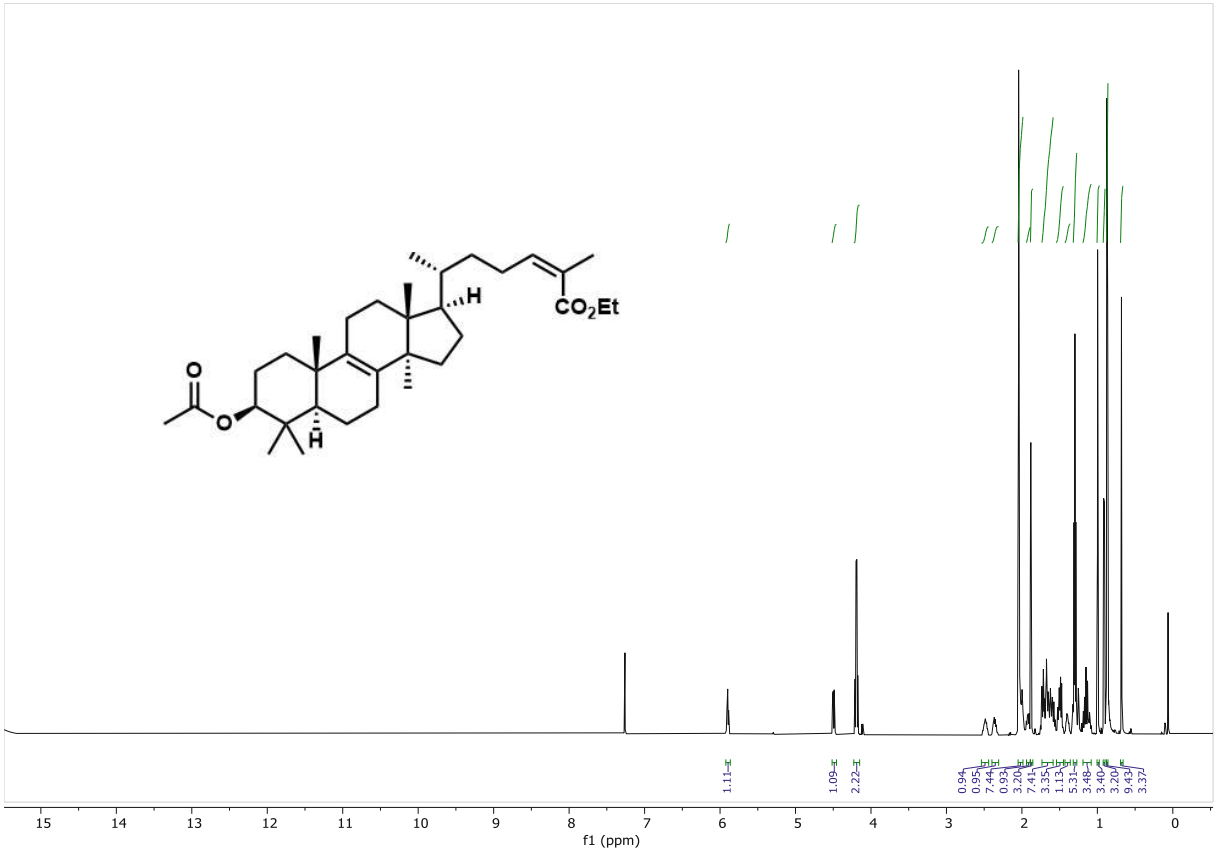

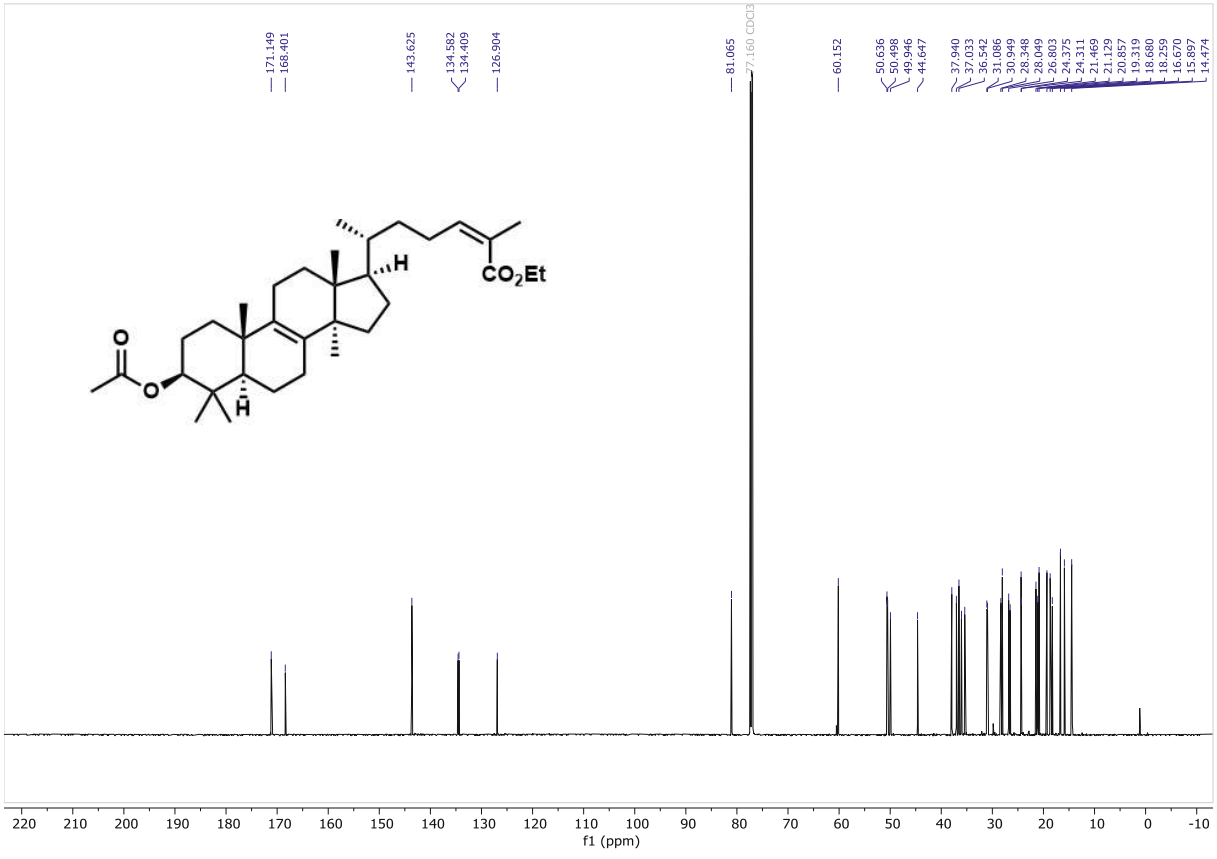

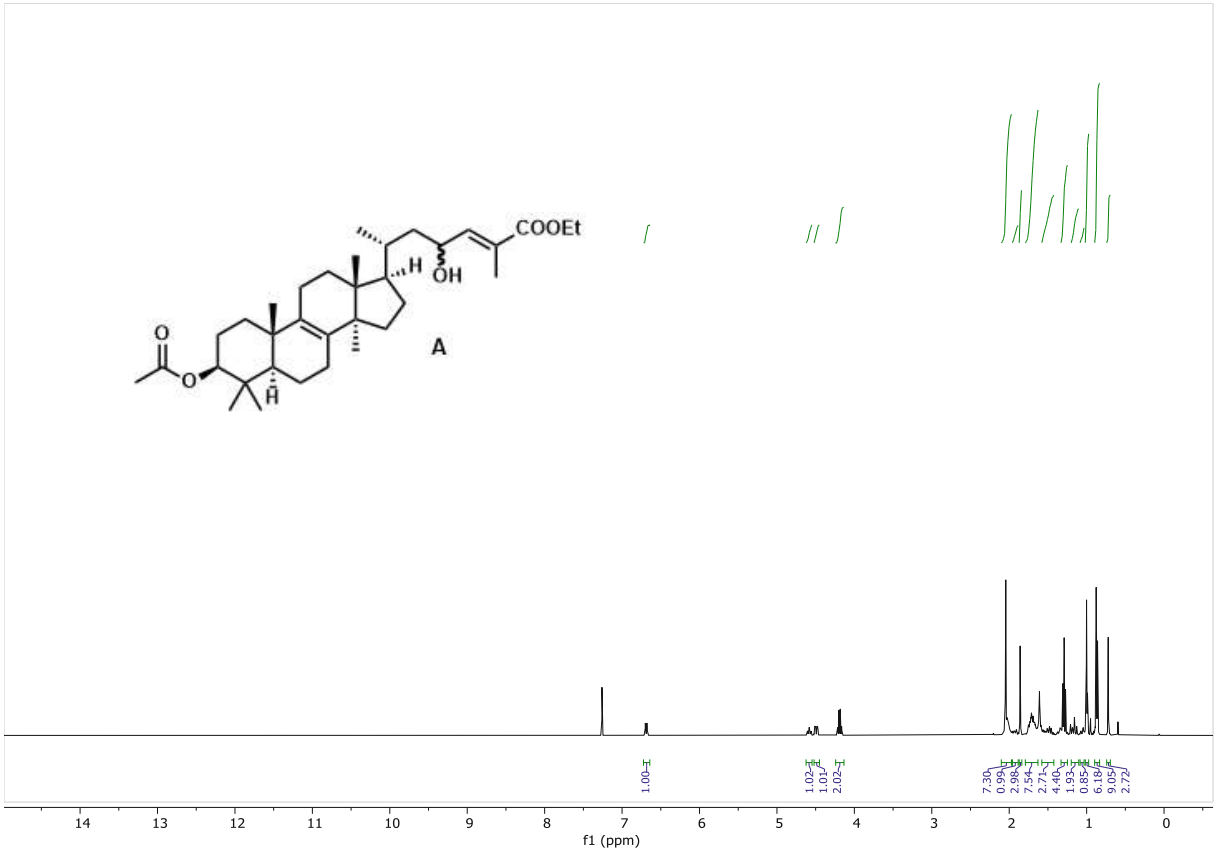

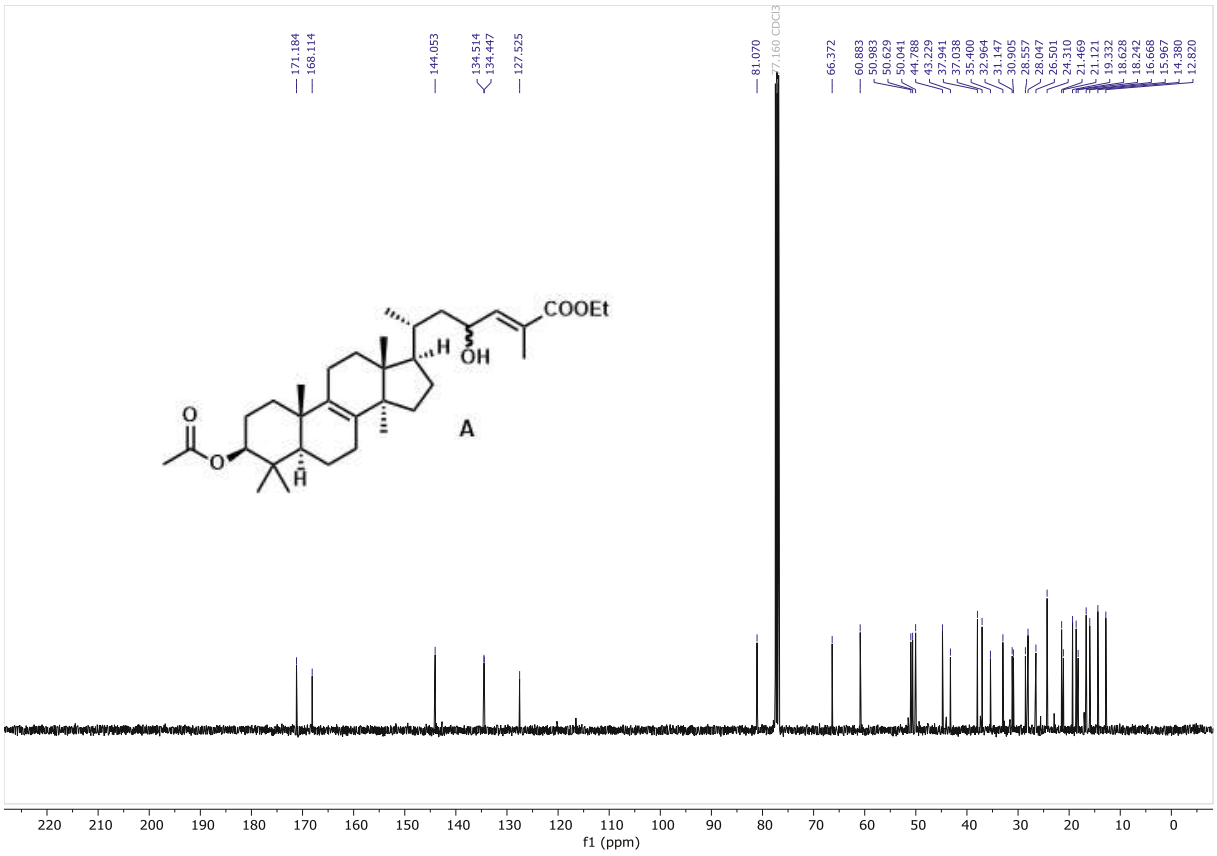

γ-OH B